1972

A yield and fracture model for TI-6AL-4V titanium and 7075-T6 aluminum

Richard L. Pendleton

A YIELD AND FRACTURE MODEL
FOR TI-6AL-4V TITANIUM
AND
7075-T6 Aluminum

BY

RICHARD LEE PENDLETON, 1935-

A

DISSERTATION

submitted to the faculty of

THE UNIVERSITY OF MISSOURI-ROLLA

in partial fulfillment of the requirements for the

Degree of

DOCTOR OF PHILOSOPHY IN MECHANICAL ENGINEERING

Rolla, Missouri

1972

Approved by

Robert L. Davis (Advisor) Glen Haddad

Jerry J. Lehnhoff J. R. Fawcett

R. O. Rocke

R. B. Oetting

ABSTRACT

The objective of the research being reported in this thesis was to conduct a series of experiments on two commonly used structural metals in several different environmental pressures so that a graphical representation of the material response both to yielding and fracture could be ascertained. It was further intended to show that parameters herein defined and called effective stress, effective strain, and pressure are useful parameters for graphically representing the material response. The final goal of this research was to show that the graphical representation does, in fact, predict the yield and fracture for a simple forming process. The forming process, conducted in various environmental pressures, was the folding of a thin plate.

ACKNOWLEDGEMENTS

The author wishes to express his sincere appreciation for the technical assistance and inspiration provided by Dr. R. L. Davis.

The author further wishes to acknowledge the invaluable assistance provided by Mr. Wilson Sherrill. In addition, the author acknowledges the efforts and patience of Dr. T. R. Faucett, Dr. T. F. Lehnhoff, Dr. A. G. Haddock, and Dr. R. B. Oetting.

The author additionally desires to acknowledge his wife, Lavon, and children, Richard, Linda, Rebecca and David for their uncomplaining patience and morale building efforts during this effort.

In conclusion this author must acknowledge the assistance of his spiritual Father whose helps are too numerous to recount.

TABLE OF CONTENTS

LIST OF TABLES

LIST OF ILLUSTRATIONS

NOMENCLATURE AND LIST OF SYMBOLS

J_1	First Invariant of the Stress Tensor
J_2	Second Invariant of the Stress Tensor
J_3	Third Invariant of the Stress Tensor
J'_2	Second Invariant of the Deviatoric Stress Tensor
J'_3	Third Invariant of the Deviatoric Stress Tensor
f	Function Describing the Yield Criterion
g	Function Describing the Plastic Potential of the Material
G	Function of the First Invariant of the Stress Tensor
H	Function of the Second and Third Invariants of the Deviatoric Stress Tensor
k, α, β	Material Constants
δ_{ij}	Kronecker Delta
σ_{ij}	Stress Tensor
σ_e	Effective Stress
P	Pressure
$\sigma_1, \sigma_2, \sigma_3$	Principal Normal Stresses
σ_x, σ_y	Normal Stress
τ_{xy}	Shear Stress
$d\varepsilon_{ij}^P$	Differential Plastic Strain Increment Tensor
ε_e	Effective Strain
$\varepsilon_1, \varepsilon_2, \varepsilon_3$	Principal Normal Strains

ε_y	Normal Strain
$\Delta\varepsilon_y^P$	Plastic Strain Increment
ksi	Thousand Pounds Per Square Inch
L/D	Length to Diameter Ratio
N	Force Per Unit Width Normal to the Cross Section
Q	Force Per Unit Width Parallel to the Cross Section
M	Internal Moment Per Unit Width about the Z Axis
L	One-Half the Length of the Beam
Θ	Angle
E	Modulus of Elasticity
Θ_o	Load Increment Factor
Θ_1	Moment Increment Factor
x,y,z	Coordinates
V	Displacement in the Y Direction
w	Displacement in the Z Direction
$\bar{V}$	Displacement of the Neutral Axis in the Y Direction
V_y	Derivative of V with Respect to Y
w_y	Derivative of w with respect to Y
w_{yy}	Second Derivative of w with respect to Y
h	Height of Beam
C_1, C_2	Constants of Integration
μ	Poisson's Ratio
h'	Function Describing Strain History of the Material

I. INTRODUCTION

Extrusion and forming of metals has been of vital interest since the earliest blacksmith. Many processes have been developed over the years for the improvement of metal forming and extrusion. The primary factors to be overcome during the forming processes are loss of ductility and loss of strength due to microscopic cracks and internal voids. In the aircraft industry the problems of forming techniques are magnified by the use of new and exotic materials for which little or no data is available, and recently at least, by the great size of the parts to be assembled. In many areas, parts that now must be slowly, laboriously, and expensively machined could perhaps be formed directly if our understanding were greater. The cracks which presently occur, and the elaborate stress relieving procedures required, often without consistent benefit, are problems which may be overcome.

Many variations in extrusion techniques have been used. Square dies, wedge shaped dies, dies with various curvatures have all had application and met with varying degrees of success. Through the work of Dr. P. W. Bridgman[1*], and his patented process using back pressure on the billet being extruded, it first became apparent that hydrostatic pressure

---

*Superscript numbers refer to similarly numbered references in the Bibliography.

can be an important factor in forming processes. His results, when compared with those procedures previously used, were almost fantastic.

The study of the phenomenon of fracture has occupied investigators in the fields of metallurgy, mechanics, civil engineering, and mechanical engineering for many years but is still only vaguely understood. Recently the works of Bridgman, Hu and Davis in the field of high pressure mechanics have provided some enlightenment and opened the doors to formulating a basic theory for the yielding and fracture of metals related to the environmental pressure of the material.

A theory presented by Dr. Davis[2] at the University of Missouri - Rolla established parameters of stress and strain which produce a functional relationship similar to the well established and much used uniaxial tension stress strain curve. This model, developed by Dr. Davis, allows the yielding and fracture of the material to be predicted regardless of the manner in which the structure is loaded. The structure may be loaded triaxially with any combination of shear and normal stresses and strains. The model has been developed for Nittany No. 2 Brass and fits the data gathered by several investigators quite well. Data has been taken from the work of Bridgman for mild carbon steel and a very similar pattern is formed for the model. Even for a nominally brittle material such as cast iron the proposed model fits the experimental data. The model is expected to be similar for most structural metals, but the exact shape must be

experimentally determined for each material. Certain characteristics of the model and its general shape can be expected to remain consistent from material to material as in the uniaxial curve and this could prove very beneficial in developing a more general theory of yielding and fracture.

The previously mentioned model is a graphical representation obtained by plotting parameters of stress versus strain versus hydrostatic pressure. The parameters of stress and strain must incorporate, in some manner, all of the stresses and strains which may exist at a point in the material so that a variation in any shear or normal stress or strain will produce a variation of the parameters. It is also important that the parameters be invariants of the stress and strain tensors so that they do not depend on the coordinate system used to describe the system. The parameters called effective stress, effective strain and pressure, which will subsequently be defined, satisfy these conditions. These quantities have been used by many investigators for various purposes and are commonly called octahedral shear stress, effective stress, or the second stress invariant of the deviatoric stress tensor; octahedral shear strain, or effective strain; and hydrostatic stress, pressure, or the first stress invariant. The effective stress is the parameter used by von Mises to indicate incipient yielding. It was necessary to determine the number of experimental tests required to establish the shape of the model for those materials which we desire to investigate. It is highly

probable that the number of tests required to construct the model will be the same for all materials, but only further experimentation will verify this.

It is believed that the model will prove useful in many ways to explain phenomena which have been observed but, much more importantly, will allow the prediction of failure, both elastic and plastic, for any combination of stresses which may be applied so that processes may be designed with relative ease for the extrusion and forming of parts. One particularly important feature of the model is that it gives a firm indication of the degree of ductility or brittleness associated with a forming process on a material. Normally it is desired that the material be as ductile as possible during the forming process to avoid the brittle cracks which may form and to allow the material to stress relieve itself as the forming loads are removed.

For the model under discussion to be of any practical value it is obviously essential that the state of stress and strain in the material be known during the forming process. Direct analytical procedures are usually too difficult to handle and even indirect techniques using the digital computer may prove extremely difficult, or in some cases not presently possible. Recently, however, a method called the finite element technique (Appendix A) has been developed which has great flexibility and application in the type of problem which is under consideration here. A computer system, using the finite element approach, allows the

prediction of the state of stress and strain in the material, and will provide directly the effective stress and effective strain for many of the forming processes that it may be desired to investigate. Many modifications of the existing finite element program have already been introduced by Dr. Davis and Dr. Keith at the University of Missouri - Rolla (UMR) to extend its application to inelastic behavior. As more modifications become available, and especially as the program becomes capable of solving problems involving large inelastic deformations, the overall design program for predicting particular forming operations for specific jobs will be greatly enhanced.

In general, there are a number of studies which must be performed in order to investigate the feasibility of designing a forming operation. These studies would include such things as die design, forming temperature, shape and size of the part to be formed, and the pressure at which the process is to take place. Two studies relevant to the research in this thesis are material behavior and stress analysis during the forming operation. The material behavior must be studied since the material response greatly influences the stress analysis. It will subsequently be shown that the reverse is also true: the state of the stress and strain also influences the material behavior. Several specifically designed tests were performed on specimens of two frequently used metals for the purpose of constructing a yield and fracture model for each material.

II. LITERATURE REVIEW

Until very recently it has been assumed by most investigators that the hydrostatic component of stress, also called the first stress invariant or pressure, contributed no influence to the inelastic behavior of materials. In classical plasticity the state of stress is divided into spherical and deviatoric components. The spherical component, which is the hydrostatic component, is neglected and all stress-strain relations are based on the deviatoric component. The yield condition of von Mises postulates that yielding, both initial and subsequent, occurs when the deviatoric component attains a particular value equal to the octahedral shear stress. The yield condition of Tresca is also independent of the hydrostatic component of stress.

The work of P. W. Bridgman[1] first created an awareness that the response of a material when tested under pressure is different than when the test is conducted in atmosphere. Bridgman's first publication in this area was in 1912, and he was the primary contributor to this field until the 1950's. In 1948 Bridgman reported a successful extrusion of a copper billet reducing the cross-sectional area by a ratio of 16 to 1 in a single pass using a pressure of 170 ksi.

Hu[3] has presented a very elegant argument on the necessity of including the first stress invariant in any yield criterion by beginning with the basic hypotheses of Hill[4] concerning yield surfaces, strain-hardening characteristics,

and plastic potential. The argument does not specify the type of relationship that exists; just that the relationship does exist. The relationship can be determined experimentally. This has been done by several investigators such as Hu, Markowitz, and Bartush[5], Davis[2] (using data from Bridgman and others) and Bobrowsky[6].

In recent years several investigators have made contributions to the field of metalworking under pressure. In the USSR, Beresnev and Vereschagin[7] have reported on working of materials at extremely high pressures. Just outside Moscow there is a laboratory with a press for producing loads up to twenty million pounds, and under construction is a one hundred million pound press, two hundred and forty feet tall with five stages of support for the pressurizing volume. This equipment, if it is successful, will operate in the pressure range of 7,000 ksi to 30,000 ksi. With their existing equipment the Russian investigators have been able to manufacture polycrystalline diamonds and fabricate sintered diamond compacts in volumes as large as one liter. Vereschagin has reported[7] that the cost of producing the sintered diamond is less than the cost of conventional cobalt bonded tungsten or titanium carbides, and a sintered diamond bit greatly outperformed conventional tool bits. Detailed information on this Russian activity is not available. Many applications to metalworking under pressure and hydrostatic extrusion have been discovered by investigators in laboratories although commercial applications are still very limited.

Pugh[8] in England, and Avitzur[9] in the U.S. have made outstanding contributions in the field of hydrostatic extrusion and have studied such parameters as friction, die angles, die design, types of fluids and their response to high pressures, and overall extrusion configuration. Bobrowsky[7] has made an enormous contribution in stimulating interest in the field with his publication of PRESSURE RESEARCH NOTES as well as producing a large amount of research.

This author feels that the macroscopic model proposed by Davis will, in time, prove to be one of the most important design tools for engineers in existence. This model when used in conjunction with computer analyses to ascertain the state of stress within a structure will enable engineers to design with confidence in the inelastic range. Hu, Hoeg[10], and Prager[11] have made theoretical and experimental contributions to the understanding of successive yield surfaces.

Metalworking under pressure is commercially successful in the production of hollow parts. This method is superior to other methods because the pressure not only increases material ductility but the forming process allows more favorable stress states, maximum bulging of the part, and a reduction in tearing of the metal. Commercially the pressure inducing medium may be a soft solid such as urethane used by Di-Acro Houdailles forming processes or liquids which are used by American Standard in the production of faucets. Western Electric has perhaps been the most progressive corporation in this area. Since 1966 they have employed the

use of internal and external pressures as well as superimposed stress in manufacturing processes and have successfully combined metal forming under pressure with metal separation such as "clean punching". Western Electric is also working on a continuous hydrostatic extrusion process. There is presently no commercially proven hydrostatic extrusion process that has been released to the public, even though Bridgman first proved the process to be feasible in 1948. In the early 1960's the Pressure Technology Corporation of America achieved a reduction in area of 2 to 1 for a 300-series maraging steel in a single pass using a pressure of 450 ksi and ASEA (Sweden)[7] has reported a reduction ratio for aluminum up to 22,500 to 1.

III. THEORETICAL CONSIDERATIONS

In the field of inelastic analysis certain assumptions based on experimental evidence are inevitable. It is certainly possible for a formulation to seem to describe known phenomena accurately and still be in error simply because those conditions which prove the error are not commonly experienced. This seems to be the case regarding Newton's Second Law of Motion which has wide application to common experience but is somewhat in error in those situations involving velocities approaching the speed of light. It is felt that the influence of pressure on the behavior of metals very closely parallels that of Newton's Law of Motion. Experimental evidence implies that the first stress invariant (J_1) can be separated from the existing state of stress and deleted from all stress, strain, displacement and yield calculations. L. W. Hu[3], using parameters described in the classic book "Plasticity" by Hill[4], has provided analytical evidence that in general yield is not, in fact, independent of J_1. If f is some function which describes the yield criterion, g is some function describing the plastic potential of the material, and h' is a function which describes the strain history or strain hardening characteristic of the material, then the plastic strain increment can be expressed in terms of these functions. If we assume that the yield criterion f is not only dependent on the conventional criterion of the second and third invariants of the deviatoric stress tensor (J'_2 and J'_3) but is also a function of the first stress invariant (J_1), the following

can be shown:

$$f = f(J_1, J'_2, J'_3) \tag{1}$$

where

$$J_1 = \sigma_{ii}$$

$$J'_2 = \frac{1}{2}\{(\sigma_{ij} - \frac{1}{3}\delta_{ij}\sigma_{kk})(\sigma_{ij} - \frac{1}{3}\delta_{ij}\sigma_{kk})\}$$

$$J'_3 = \frac{1}{3}\{(\sigma_{ij} - \frac{1}{3}\delta_{ij}\sigma_{kk})(\sigma_{jk} - \frac{1}{3}\delta_{jk}\sigma_{ii})$$

$$(\sigma_{ik} - \frac{1}{3}\delta_{ik}\sigma_{jj})\}$$

and σ_{ij} is the stress tensor. From Hill[12] we obtain the following relationship:

$$d\varepsilon_{ij}^{P} = h'(\sigma_{ij})\ \frac{\partial g}{\partial \sigma_{ij}}\ df \tag{2}$$

where $d\varepsilon_{ij}^{P}$ is the plastic strain increment. No one has discovered the relationship between the plastic potential (g) of a material and the yield surface (f), but it is very useful and common to assume g = f for the purpose of analyzing the nature of the function f using variational principals and uniqueness theorems. With this substitution into Equation 2 we can obtain:

$$d\varepsilon_{ij}^{P} = h' \frac{\partial f}{\partial \sigma_{ij}} \, df \, . \tag{3}$$

Mathematically it is reasonable to assume that f is of the following form:

$$f(J_1, J'_2, J'_3) = G(J_1) \, H(J'_2, J'_3) \, . \tag{4}$$

This form is not only permissible mathematically but is in fact shown to be valid by the experimental results of this thesis. With this substitution Equation 3 becomes:

$$d\varepsilon_{ij}^{P} = h'\{G \frac{\partial H}{\partial \sigma_{ij}} + \delta_{ij} \, H \frac{\partial G}{\partial \sigma_{ij}} \} \, df \tag{5}$$

By definition the function G is independent of the second and third deviatoric invariants and therefore:

$$\frac{\partial G}{\partial \sigma_{ij}} = \frac{dG}{dJ_1} \tag{6}$$

$$d\varepsilon_{ij}^{P} = h'\{G \frac{\partial H}{\partial \sigma_{ij}} + \delta_{ij} \, H \frac{dG}{dJ_1} \} \, df \tag{7}$$

A common assumption in inelastic analysis is that of volume constancy which can be expressed equivalently using the expression

$$d\varepsilon_{ii}^{P} = 0 \ . \tag{8}$$

$$d\varepsilon_{ii}^{P} = h'\{G \frac{\partial H}{\partial \sigma_{ii}} + \delta_{ii} H \frac{dG}{dJ_1}\} df \tag{9}$$

$$d\varepsilon_{ii}^{P} = 3 Hh' \frac{dG}{dJ_1} df \ . \tag{10}$$

There are only two conditions possible for volume constancy if this formulation is correct. Volume constancy is valid if $H = 0$. This of course implies that $J'_2 = J'_3 = 0$. This is only true in a case of pure hydrostatic stress. Volume constancy is also valid if $G = 0$ which implies that $J_1 = 0$ which is a case of pure shear. It is apparent that for a general state of stress the volume is not constant during inelastic deformation. Rather than proving objectionable this conclusion has been supported by experimental evidence[13,14].

The preceeding development assumed that the yield criterion was a function of J_1. Let us investigate, mathematically the validity of incorporating the first stress invariant into the yield criterion f. This can be done very neatly by assuming that $f = f(J_1, J_2, J_3)$ where J_1, J_2, and J_3 are the first three stress invariants. At the onset of plastic flow the following relationship must be valid for all strain hardening materials:

$$df = \frac{\partial f}{\partial J_1} d J_1 + \frac{\partial f}{\partial J_2} d J_2 + \frac{\partial f}{\partial J_3} d J_3 > 0$$

If the case of uniaxial tension or compression is considered we have the following:

$$\sigma_{xx} = \pm \sigma \qquad \sigma_{yy} = \sigma_{zz} = \sigma_{xy} = \sigma_{xz} = \sigma_{yz} = 0$$

therefore

$$J_1 = \pm \sigma \qquad J_2 = J_3 = 0$$

and

$$df = \frac{\partial f}{\partial J_1} d J_1 > 0 \ .$$

It is obvious, therefore, that yielding is a function of J_1 if $f = f(J_1, J_2, J_3)$. This is not, of course, a rigorous mathematical proof, but it is a strong indication that the first stress invariant must not be deleted from the yield criterion without very powerful reasons for doing so. The primary reason this has commonly been assumed is because of the gain in analytical simplicity and because, until quite recently, experimental evidence failed to discern the dependency of the yield criterion on the first stress invariant.

An interesting formulation suggesting a compromise between the two theories

$$f = f(J'_2, J'_3) \quad \text{and} \quad f = G(J_1)\ H(J'_2, J'_3)$$

has been proposed by Hu and Pae[15]. If plastic deformation is a function of the stress deviators J'_2 and J'_3, but the effectiveness of the deviators is subject to an influence of J_1, the yield condition could be written in the form:

$$f = \sum a_i\ J_1^{\,i}\ .$$

A simple form of this would be

$$f = k^2 + \alpha\ J_1 + \beta\ J_1^{\,2}$$

where k, α, and β are material constants. It has been shown that this formulation does describe much of the observed phenomena concerning pressure, but it is doubtful that it will gain very wide acceptance for purposes of computations due to its complexity especially in problems involving elastic-plastic interfaces.

Since any arbitrary stress state can be specified in terms of three principal values (σ_1, σ_2, σ_3) it is useful to work in terms of these values. It is extremely useful to establish a coordinate system where the three principal stresses are taken as the cartesian coordinates in a three

dimensional space. The Pi plane is a plane in this space defined by the equation

$$\sigma_1 + \sigma_2 + \sigma_3 = 0 \ .$$

The pressure axis is defined as perpendicular to the Pi plane and has direction cosines of $(1/\sqrt{3}\ ,\ 1/\sqrt{3}\ ,\ 1/\sqrt{3})$. For an isotropic material it is obvious that the yield locus must be symmetric with respect to the principal stress axes, and since the stress component which lies in the Pi plane fulfills this condition it is commonly used as a yield criterion. This criterion has been developed in several different ways and, therefore, is called different names such as effective stress, octahedral shear stress, second deviatoric stress invariant, and von Mises yield condition. The effective stress is given by the equation:

$$\sigma_e = \frac{1}{\sqrt{2}} \left\{ (\sigma_1 - \sigma_2)^2 + (\sigma_2 - \sigma_3)^2 + (\sigma_3 - \sigma_1)^2 \right\}^{1/2}$$

The second component of stress which lies parallel to the pressure axis is ordinarily assumed to have no influence on the yield locus so that the yield locus would be a right circular cylinder with generators perpendicular to the Pi plane and a radius corresponding to the effective stress. Since, for an isotropic material, the yield surface must be symmetric in the Pi plane it is evident that the cross section

of the yield surface must be circular so that if the pressure has an influence it must be that of inducing a conical shape to the yield locus. It is well known that all materials, even those which were initially isotropic, become anisotropic after yielding so that successive yield surfaces, or post yield surfaces, would not be limited to circular cross sections in the Pi plane. Hill[2] has an excellent discussion on the general nature of the yield locus. Hoeg[10] has investigated the nature of the post yield surface and shows it to be nearly circular with an expanded radius and a shift of the origin in the direction of prestrain.

The strain matrix is not related to a yield locus by most investigators. This is probably due to one of two reasons. Some investigators feel it is sufficient to relate the yield locus to the stress state and the strain state to the stress state thereby describing the inelastic material response. The second reason for not including the strain matrix in describing the yield locus is simply that we have not known how to do so. The problem is admittedly complex since it requires satisfying the conditions of symmetry, invariance, and generality of describing all load and strain paths while coupling the stress and strain together. The effective shear strain is given by the equation:

$$\varepsilon_e = \frac{\sqrt{2}}{2(1+\mu)} \left\{ (\varepsilon_1 - \varepsilon_2)^2 + (\varepsilon_2' - \varepsilon_3)^2 + (\varepsilon_3 - \varepsilon_1)^2 \right\}^{1/2}$$

where μ is Poisson's Ratio and ε_1, ε_2, and ε_3 are principal

strains. In the plastic region μ is normally assumed to be .5 and the effective strain is

$$\varepsilon_e = \frac{\sqrt{2}}{3} \left\{ (\varepsilon_1 - \varepsilon_2)^2 + (\varepsilon_2 - \varepsilon_3)^2 + (\varepsilon_3 - \varepsilon_1)^2 \right\}^{1/2}$$

ε_e is both symmetric and invariant, and is the strain parameter used in this thesis. It is felt by the author of this thesis that the parameters and the technique proposed by Davis[2] will prove to be of inestimable value in filling this void.

IV. DESCRIPTION OF TEST EQUIPMENT

Two materials were selected for investigation on the basis of application to industry. The materials chosen were 7075-T6 aluminum and Ti-6AL-4V titanium which are very common in the aircraft industry. A substantial quantity of these materials were furnished and specimens machined by McDonnell-Douglas Corporation in St. Louis. Three basic load configurations were used; uniaxial tension, uniaxial compression, and folding of thin plates. These tests were conducted within a pressure vessel at a number of different pressures. These tests were selected for several reasons. It was necessary that the basic configuration of the test be relatively simple because the tests were to be conducted inside a sealed chamber three inches in diameter and twelve inches high. The only loading mechanism available was a ram which extended through seals from the top of the vessel to the internal chamber. The ram could only move vertically. The tension and compression tests represent widely divergent load paths on the proposed stress versus strain versus pressure curve which allowed the model to be more completely defined than if only tension or only compression tests were conducted. The bending or folding of the plates was selected because it provided a check on the tension and compression data since the plate will be in tension on one side and in compression on the other. In addition the folding of the plate would determine qualitatively whether or

not the presence of environmental pressure will increase the amount that the plates can be folded prior to fracture.

In order to conduct the experimentation certain equipment was necessary (Fig. 1 and Fig. 2). A pressure vessel capable of containing 125 ksi was purchased from Harwood Engineering. A positive displacement pump was purchased which was capable of delivering 125 ksi. A manganin pressure cell capable of measuring pressures up to 250 ksi and a bourdon pressure gage capable of measuring pressures up to 100 ksi were obtained for monitoring the pressures. A large number of post yield foil strain gages were purchased, and the specimens were furnished by the McDonnell-Douglas Corporation. A fork lift to position the pressure vessel in the Riehle Compression Tester was obtained from government surplus. The Riehle Compression Tester was adapted so that the pressure vessel would fit between the compression heads (Fig. 2). The compression tester available had a capacity of 300 kips which was more than adequate for this series of tests.

For most of the tests conducted it was desired to monitor and record the pressure in the vessel, the load exerted on the ram by the Riehle Compression Tester, a load cell strain, and a specimen strain. The last two strains were measured using the post yield foil electrical strain gages. A special testing module was designed for each of the three types of tests which were conducted. With the exception of containing different testing modules, each of the tests

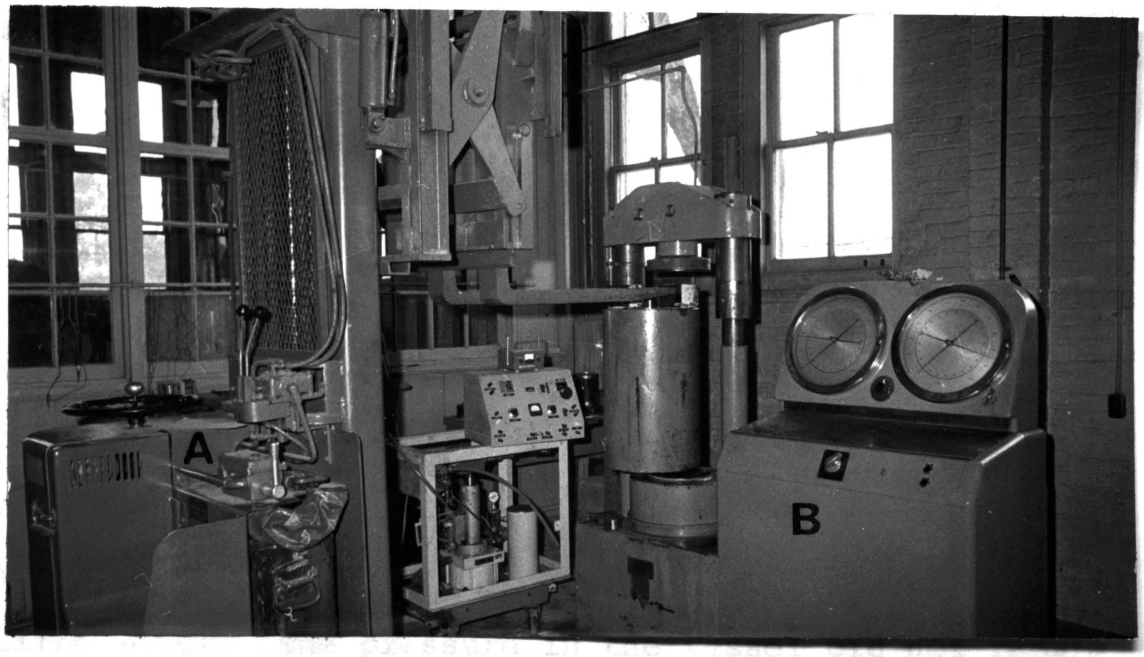

A - Fork Lift B - Compression Tester

Fig. 1 Test Equipment with Fork Lift

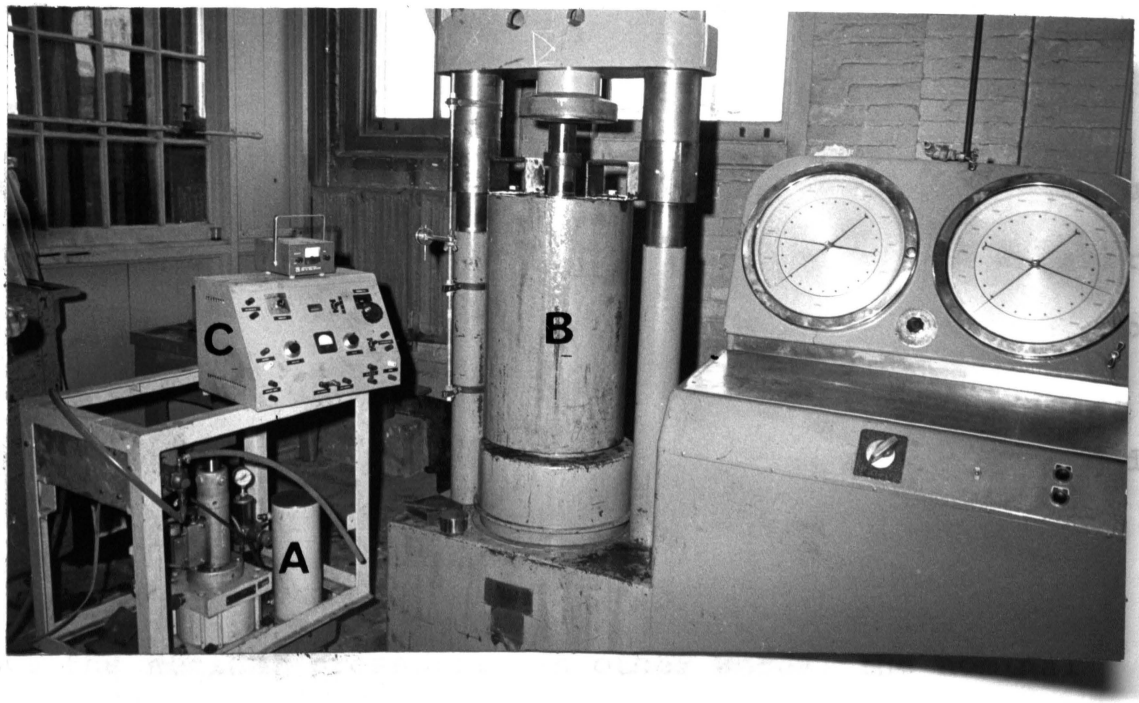

A - 125 ksi Pump B - 125 ksi Pressure Vessel

C - Manganin Cell

Fig. 2 Pressure Vessel, Manganin Pressure Cell and Reihle Compression Tester

were conducted in essentially the same manner. The module was placed in the vessel and the vessel was capped with the top seal ring and the top seal plug. The vessel was filled with hydraulic oil and the loading ram put in place. The vessel was then lifted into the Reihle Compression Tester using the fork lift. Next an initial load was applied to the ram to keep it in position while the pressure in the vessel was pumped to the desired level. The hydraulic pump was then connected and the pressure brought to the desired level. The pressure in the vessel did not remain constant during the tests but varied from two thousand psi to ten thousand psi depending on the type of test being run and the pressure at which the test was being conducted. For example, the pressure variation was very small during a thirty thousand psi compression test because the ram displacement during the test was relatively small. The pressure variation during a ninety thousand psi tension test however was approximately ten thousand psi. It was not possible to control this fluctuation of pressure so a compromise was made. The initial pressure was about one-half the expected fluctuation less than the nominal pressure, therefore, the final pressure would be one-half the expected fluctuation above the nominal pressure. In other words, the nominal pressure was actually the mean pressure. When the desired pressure level had been obtained, the ram was pushed into the pressure vessel thereby exerting a load on the specimen. The loads were increased in increments selected by the

investigator, and the parameters previously mentioned were recorded until the specimen fractured or until the maximum load attainable with this system had been reached. The load limits were different for the different types of tests and will be discussed in the following section.

V. TESTING MODULES

A. Tension Test Module

To convert the downward movement of the ram into a tensile load on the specimen required a special yoke arrangement (Fig. 3A, Fig. 3B, Fig. 3C). Each specimen was seven inches long with tapered conical ends and was one-half inch in diameter. The yoke mechanism consisted of the following parts.

(a) Outer cylinder: the outer cylinder was a right circular cylinder eight inches high with a wall thickness of one-eighth inch.

(b) Inner cylinder: the inner cylinder was designed with sector shaped prongs on one end and a circular cylinder four inches high on the other. The sector shaped prongs fit openings in the top chucks, and the bottom of the cylindrical end contains a circular hole to hold the bottom chucks.

(c) Top cap: the top cap is a circular cylinder which rests on top of the prongs of the inner cylinder. The ram pushes on the top cap and transmits the load through the prongs to the bottom of the inner cylinder and thereby to the bottom of the tension specimen.

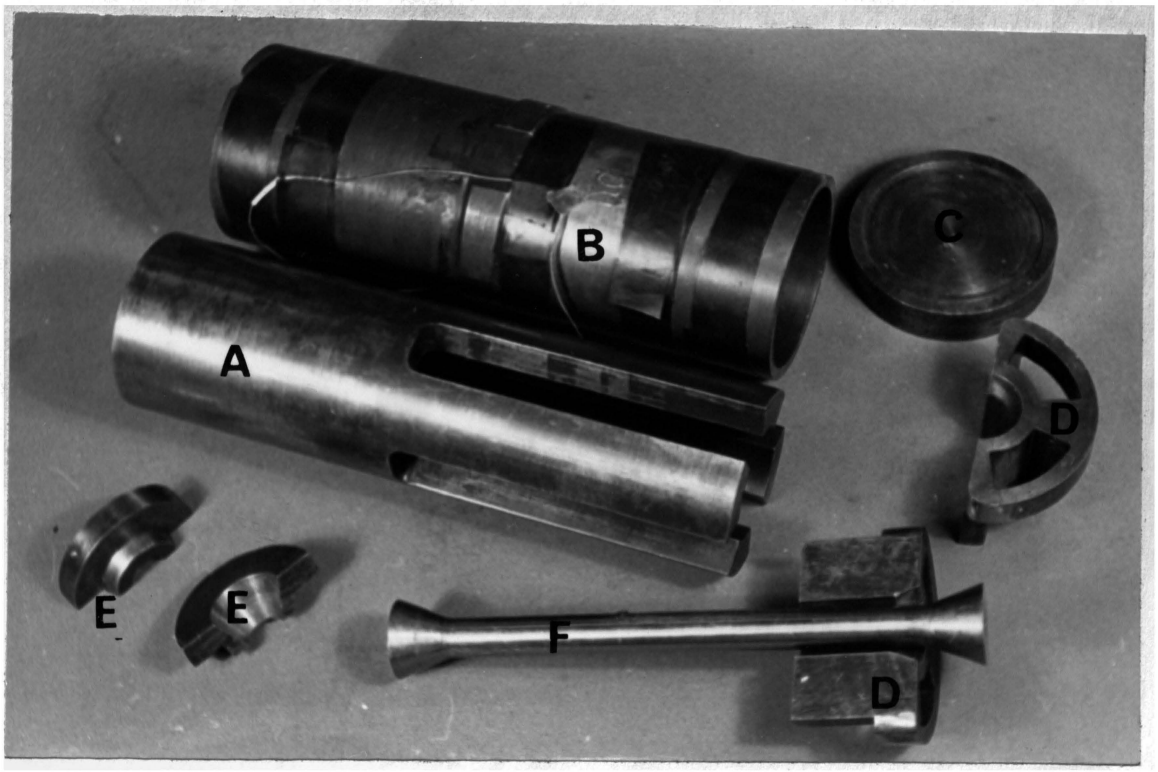

A - Inner Cylinder

B - Outer Cylinder

C - Top Cap

D - Top Chucks

E - Bottom Chucks

F - Tension Specimen

Fig. 3A Disassembled Tension Module

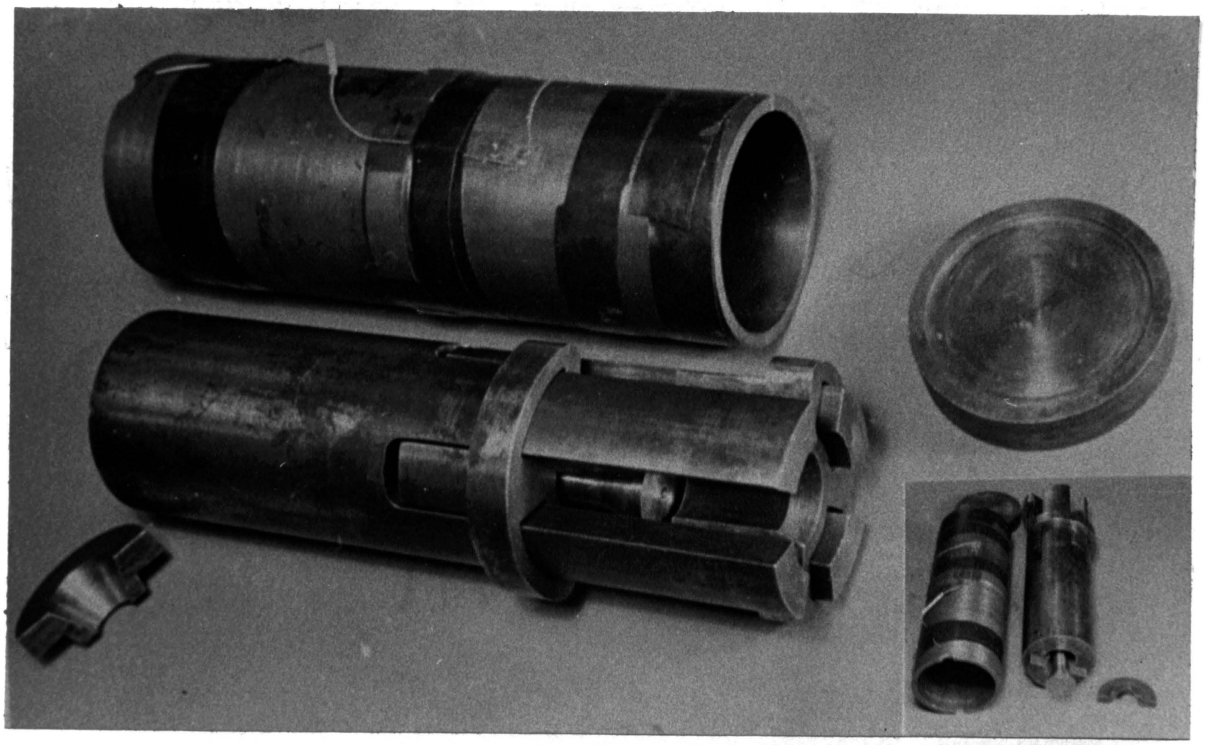

Fig. 3B Partially Assembled Tension

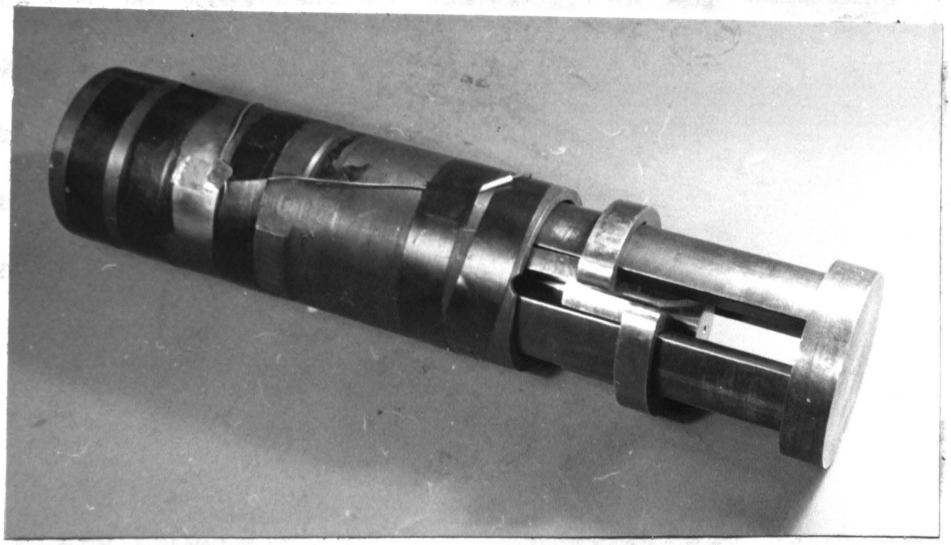

Fig. 3C Assembled Tension

(d) Top chucks: the top chucks contain openings for the sector shaped prongs of the inner cylinder and a rim which rests on the outer cylinder. The two top chucks have a one-half inch diameter hole in the center just below a tapered conical portion which fits the top of the tapered specimen.

(e) Bottom chucks: the bottom chucks are two small wedge shaped pieces which fit between the cylindrical hole in the bottom of the inner cylinder and the tapered cylindrical bottom end of the specimen to hold the tension specimen in place at the bottom of the inner cylinder.

Two strain gages were attached to the outer surface of the outer cylinder to act as a load cell. Two gages were used because when they were connected in series they cancelled out any strain due to bending of the outer cylinder due to unsymmetric loading, if any existed, consequently, the load cell calibration curve was linear.

The tension module consisted essentially of a device which held the top of the specimen, using wedges, at the top of an outer cylinder while a load was applied to the bottom of the specimen by pushing on the inner cylinder. The maximum deformation which could be obtained with this module was 1.25 inches which was adequate for all of the tension tests conducted on the two materials being discussed in this thesis.

The tension tests were conducted at various pressures on both the aluminum and the titanium. For aluminum the pressures chosen were atmospheric, 40 ksi and 70 ksi. For titanium the pressures chosen were 0 ksi, 40 ksi, 60 ksi and 80 ksi. It was possible to test at the higher maximum pressure on the titanium because it was less ductile at all pressures than the aluminum. At the higher pressure the aluminum specimen deformed more than the allowable range of the tension module before fracture.

It was found during the tension testing that the load cell strain gages were not necessary. It was initially thought that the load cell was necessary because the ram load, which was read directly from the Riehle Compression Tester, was composed of three components. These components were: a force required to counteract the load from the pressure on the ram from inside the vessel; a friction load from the seals in the vessel; and the specimen load. It was discovered during the testing program that the variation in load due to pressure variation and friction variation were repetitive and correction factors were obtained. Because of this it was possible to obtain a check on the load. This fact was observed for all three types of test, and consequently a check on applied load was obtained for all of the data discussed in this thesis.

Initially it was planned to obtain information on Poisson's ratio by measuring both longitudinal and lateral strains using a two element rosette. This was ultimately

discarded because of instrumentation difficulties. The number of lead wires passing from the interior of the vessel to the outside of the vessel was sufficient to measure strains from only two gages. The knowledge and instrumentation are now available to correct that limitation and further research could be now conducted to study the variation in Poisson's ratio due to varying environmental pressure. There has been an indication of such a variation in Nittany No. 2 brass in work done by Mr. Curtis Dennis in the Engineering Mechanics Department of the University of Missouri - Rolla, but more work needs to be done before this can be accepted as fact.

B. Compression Module

The downward movement of the ram obviously was directly applicable to compression tests. A compression test module (Fig. 4A, Fig. 4B, Fig. 4C) was used for two purposes. An internal load cell was desired and it was also necessary to have assurance that the load was centrically applied to the specimen. The compression assembly consisted of a spacer cylinder to position the basic assembly in the top portion of the test chamber, a load cell, an inner ram, and an outer centering cylinder. The load cell was shaped like a spool standing on end. Two strain gages were attached 180^{o} apart on the lateral surface of the small portion of the spool and connected in series to cancel out any readings due to bending resulting from an eccentric load on the spool. The outer cylinder centered the entire assembly with respect

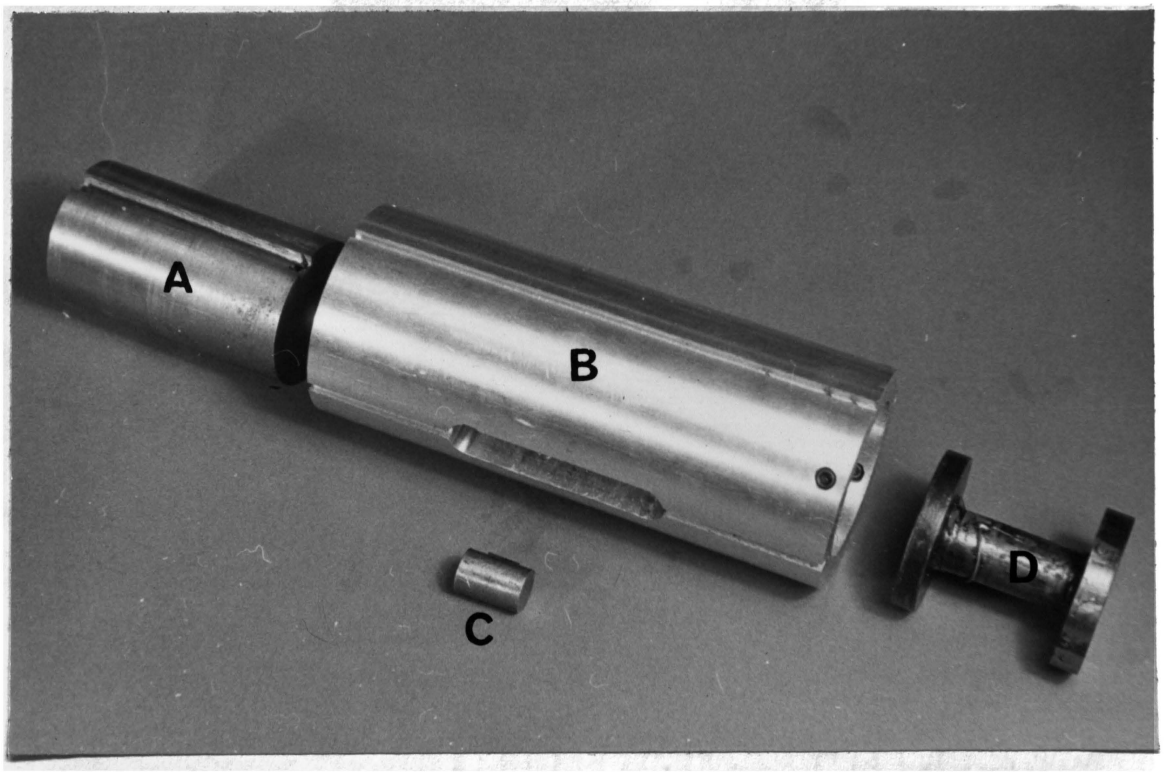

A - Inner Ram

B - Spacer Cylinder

C - Specimen

D - Load Cell

Fig. 4A Disassembled Compression Module

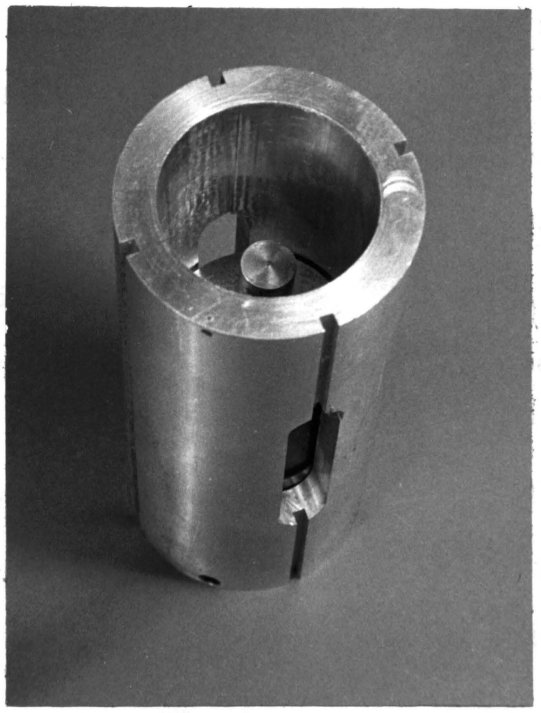

Fig. 4B Partially Assembled Compression Module

Fig. 4C Assembled Compression Module

to the vessel and the ram. The compression module functioned as desired. The compression specimen was placed in the assembly resting on the load cell. The hardened internal ram was placed in the assembly and rested on the specimen, thus securing it in place. The assembly was then placed in the pressure vessel and the pressure vessel placed in the testing machine.

Even though the application of compressive loads to the specimen presented few difficulties, the compression data and the reduction of that data to useful engineering parameters proved to be the most difficult of the three types of tests which were conducted. Initially it was planned to test cylindrical specimens with an L/D ratio of four. It was found that buckling occurred prior to fracture. A subsequent investigation indicated that an L/D ratio of 1.5 was required so that fracture would occur prior to buckling. A larger L/D than 1.5 was possible for the atmospheric tests, but was not acceptable for the tests run in a high pressure environment due to the increased ductility of the material under pressure. Substantial difficulty was encountered when attempting to bond the strain gages to the specimens so that they would transmit large strains. Strains as large as five or six per cent could be obtained, but when the specimen began barrelling noticeably the bond would fail. Measurement of large inelastic strains was finally abandoned for the compression test series because of these technical difficulties and because of theoretical

problems as well. This investigator has been unable to resolve the problem of converting the applied load to a satisfactory parameter of stress, or converting the deformation into a satisfactory parameter of strain. It is apparent that many previous investigators[16,17] have encountered similar problems without arriving at suitable solutions. The primary difficulty arises from the barrelling of the specimen under compressive loads due to friction at the ends. The friction produces a noncylindrical specimen in which both stress and strain vary from point to point. The shape of the specimen, and consequently the stress and strain distribution within the specimen, is a function of the load, and the nature of these distributions for large inelastic deformations is not known. Because of these difficulties the data has been reported in terms of the parameters of load and the total deformation divided by the current length. Yield information was easily obtained by conventional means of calculating stress and strain since barrelling does not become significant until well past yield. Despite the difficulties mentioned, the compression tests produced valuable information by (1) indicating a variation in the yield strength at varying environmental pressures, by (2) producing curves along a different load path than the other two types of tests, and by (3) the indication of a large influence on ductility at fracture that an increase in environmental pressure produces. Even though this influence could not be reported on a stress or strain basis it has

been reported on the basis of the total deformation at fracture.

C. Bending Module

It was desired to bend plates of maximum size possible through as large a deformation as possible. The three-inch diameter test chamber created the primary limitation on size. The plates tested were three inches high by two and thirteen-sixteenths inches wide and thicknesses of one-sixteenth inch, one-eighth inch and three-sixteenths inch. The bending assembly (Fig. 5A, Fig. 5B, Fig. 5C) was actuated by a hydraulic pressure system. The loading ram acted as a piston moving into a hydraulic cylinder. The pressure actuated two telescoped pistons which expand horizontally. A loading bar, moved by the telescoped pistons, impinged on the plate producing a line load along the center of the plate. The plate was simply supported along the two edges parallel to the line load. A strain gage was bonded to the upper hydraulic cylinder for use as a load cell. A great deal of effort was required to stop leakage in the system, but after these problems were solved the apparatus functioned as desired.

The plate was assembled in the bending tester and the strain gage lead wires attached. The hydraulic system was filled with hydraulic fluid and a plunger was used to expand the pistons so the plate was held snugly in place. The assembly was then placed in the pressure vessel and the pressure vessel was placed in the Riehle Compression Tester.

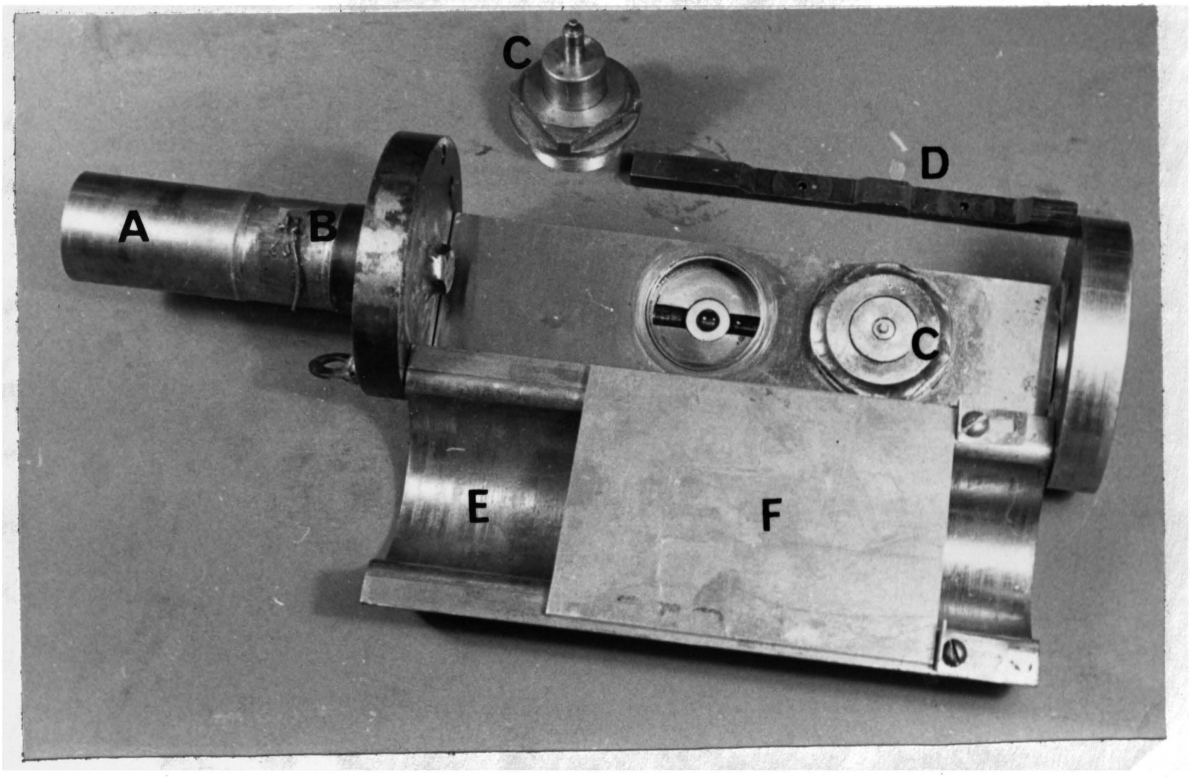

A - Hydraulic Cylinder

B - Load Cell

C - Telescoped Pistons

D - Loading Bar

E - Specimen Support

F - Bending Specimen

Fig. 5A Disassembled Bending Module

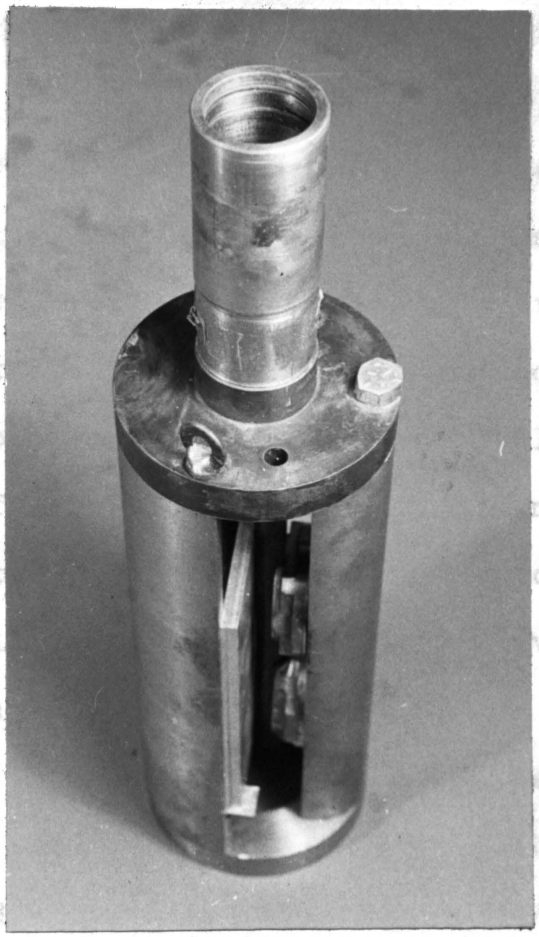

Fig. 5B Bending Module, Hydraulic Cylinder

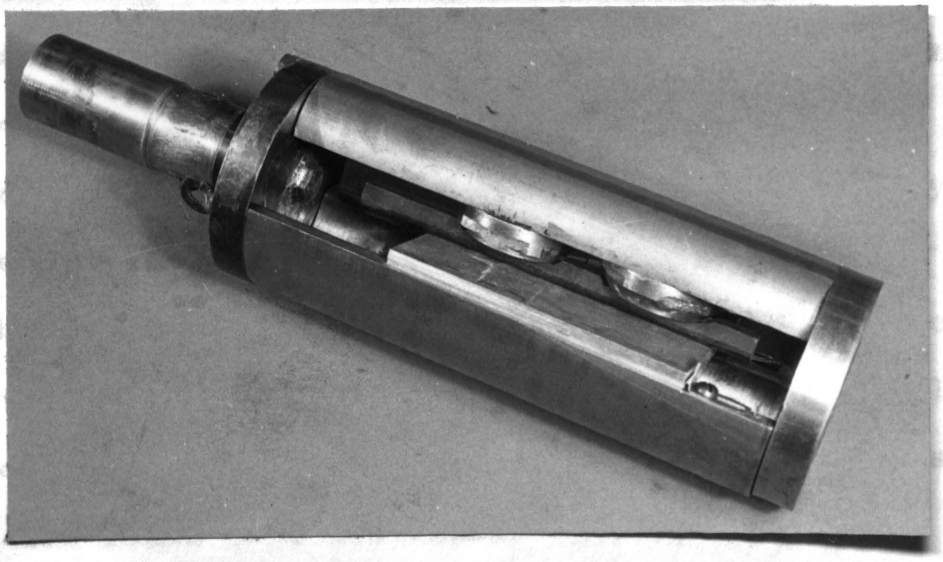

Fig. 5C Assembled Bending Module

While the fluid in the pressure vessel was raised to the desired level the ram was held in a position outside the hydraulic cylinder so the pressure inside the hydraulic system was equal to the vessel pressure. When the desired vessel pressure was reached the ram was lowered into the hydraulic cylinder providing the pressure required to expand the telescoped pistons and load the plate.

The series of tests involving the folding of rectangular plates yielded much valuable information concerning the increase of ductility with an increase in environmental pressure. Even though titanium and aluminum plates of all thicknesses could be fractured in an atmospheric environment, it was found that even at low pressures of 20 ksi the one-sixteenth inch and one-eighth inch thick plates deformed beyond the range of the bend tester without fracture. The magnitude of the strains measured during the bending tests were very large, ranging up to sixteen per cent. It was possible to compare the ductility of the plates tested in various environmental pressures by three methods. In most cases the strain gages measured strains virtually to fracture so the strain at fracture could be estimated with reasonable reliability. The total permanent deflection of the plates at fracture was easily measured after the load was removed and the plate taken from the pressure vessel. It was also found that the radius of curvature at the center of the deformed plate was directly related to the strain at fracture, and provided a means of comparing the

ductility. It is shown elsewhere that the strains predicted by the curvature and the strains obtained using strain gages were in agreement to within at least thirteen percent for the various plates tested.

VI. INTERPRETATION OF EXPERIMENTAL RESULTS

A. Titanium

(1) Tension - Tension tests were conducted on titanium specimens at environmental pressures of 0 ksi, 40 ksi, 60 ksi, and 80 ksi (Fig. 6). Within experimental accuracy there was no alteration of either the modulus of elasticity or the yield point of the material due to environmental pressure. The modulus of elasticity in tension for each of the tests conducted was calculated to be seventeen million psi, and the yield point stress was 151 ksi. Subsequent to yielding, the stress-strain curves overlapped up to fracture. When plotting the original data there seemed to be a slight divergence of the curves with the slope being slightly more positive for successively higher pressures. Corrections to the curves were applied to account for the pressure variation during the tests at higher pressures which produced curves which overlay each other. This same characteristic was observed in both the compression tests and the bending tests. A remarkable characteristic of the titanium tension family of curves was their essentially bilinear appearance. The bilinear nature of this curve would simplify a finite element computer analysis

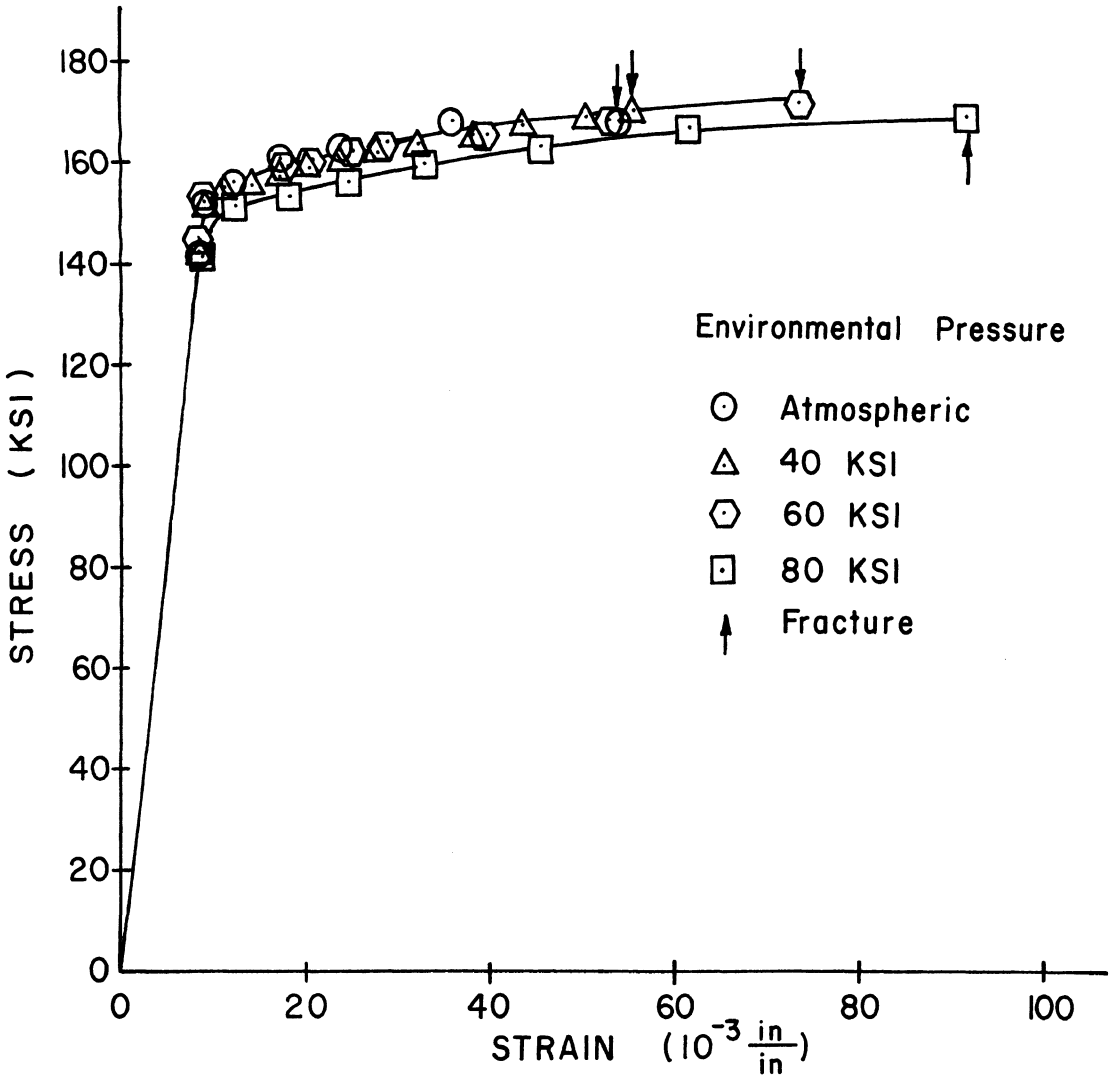

FIG. 6 TENSION TEST (TITANIUM)

of a structure made of this material. The response of this material in the plastic range was very linear for all of the tests conducted regardless of the environmental pressure or the load path. In tension only, however, there was, at yield, a very sudden, almost instantaneous, transition from elastic behavior to inelastic behavior. It is apparent from an examination of the tensile stress-strain curve that the magnitude of both stress and strain obtained at fracture is increased by testing in a pressure environment.

(2) Bending - Bending tests were conducted in environments of 0, 40 ksi, and 60 ksi (Fig. 7). The general nature of the load strain curve is similar to that of the tension stress-strain curve. It was felt that load should be a better graph parameter than stress for the folded plate since the load on the plate could be directly read with good accuracy while the stress in the plate at the location of the strain gage is not precisely known, especially after large plastic deformations have occurred. Simple beam theory was used to calculate the stress in the plate at yield, and it was assumed that the effective stress load path remained constant to fracture so that the effective stress at fracture could easily be predicted. This assumption was

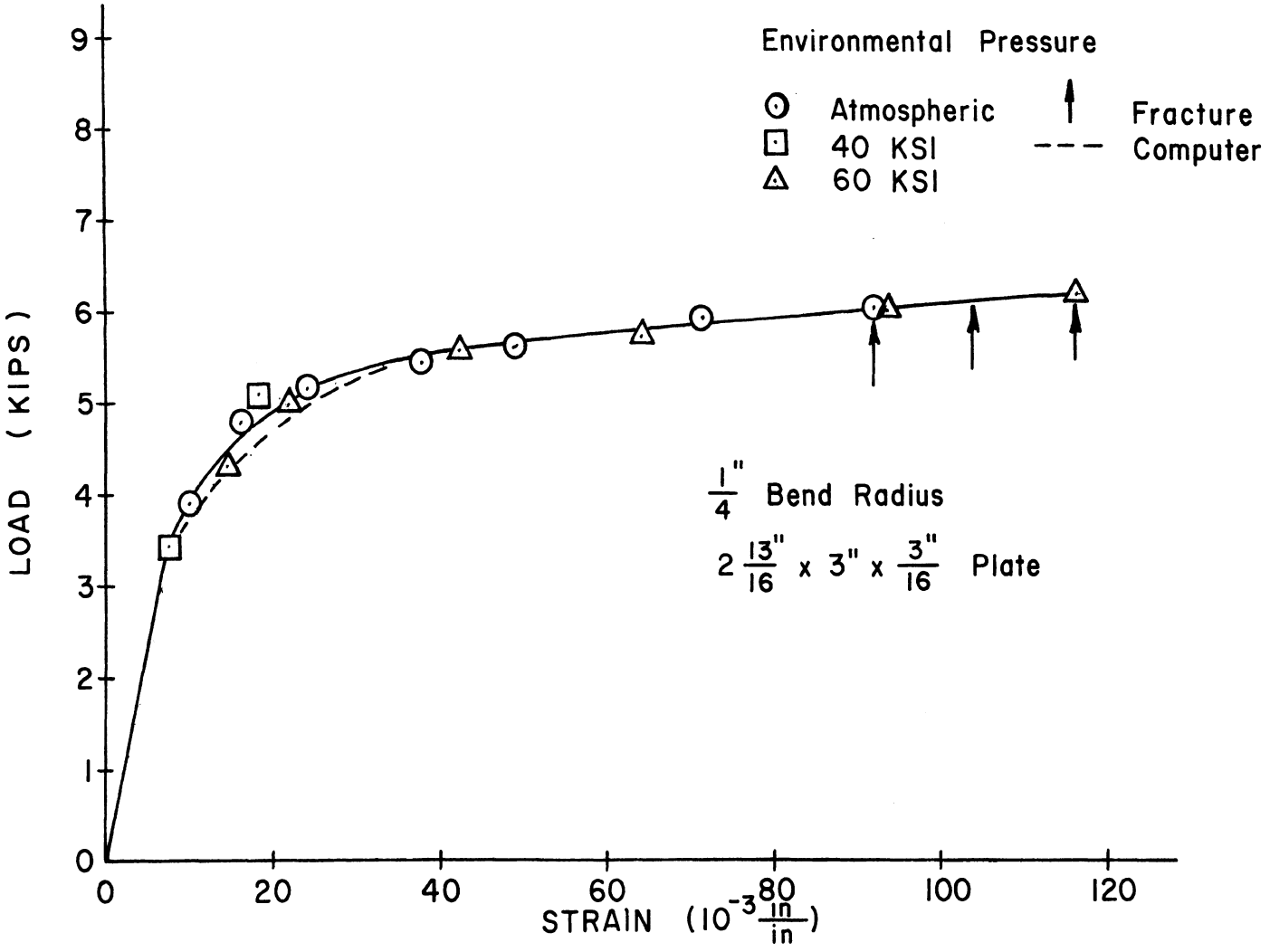

FIG. 7 BENDING TEST (TITANIUM)

substantiated when it was found that the fracture line indicated by the bending tests coincided with the fracture line indicated by the tension tests on the effective stress versus pressure graph.

The load-strain curves were independent of environmental pressure until just prior to the fracture load of the specimen loaded in an environmental pressure of 0 ksi. At this point the specimens loaded in environments of 40 ksi and 60 ksi indicated a slightly increased slope. It was not possible to ascertain whether this was due to an increasing environmental pressure during the test, which did occur, or whether this is a true material response. It seems probable to the author of this thesis that an alteration of the stresses in the plate due to excessive deformations would reflect the curve the other way, that is, the moment arm would be shortened and an additional transverse load would be significant after the plate had been folded through an angle of thirty or forty degrees. A rigorous mathematical analysis to determine the degree of influence of these parameters would be extremely difficult.

A finite element program was used to analyze the plate and the results of the computer

program agreed with the experimental data up to a load of 5,200 pounds which is a factor of 1.46 times the yield load. Fracture occurred at a load of 6,080 pounds for the specimen tested in an atmospheric environment.

(3) Compression - Compression tests were conducted at environmental pressures of 0 ksi, 20 ksi, 30 ksi, and 40 ksi (Fig. 8). Parameters of load and deformation per current length were graphed. Until the specimen yields, the state of stress and strain is uniform and easily determined. Shortly after yield, the specimen begins barrelling and the effective stress and strain are not uniform and, especially after the deformations become large, not known. Attempts were made to determine the state of stress and strain in the compression specimens using a finite element computer technique. This was relatively easy for small deformations, but the unknown shear loads on the ends of the compression specimens and the moving boundaries resulted in solutions which differed from the experimental data shortly after barrelling became significant. There are numerous methods proposed in the literature for the reduction of the friction between the compression specimen and the compression anvils, but none of them are very effective nor are

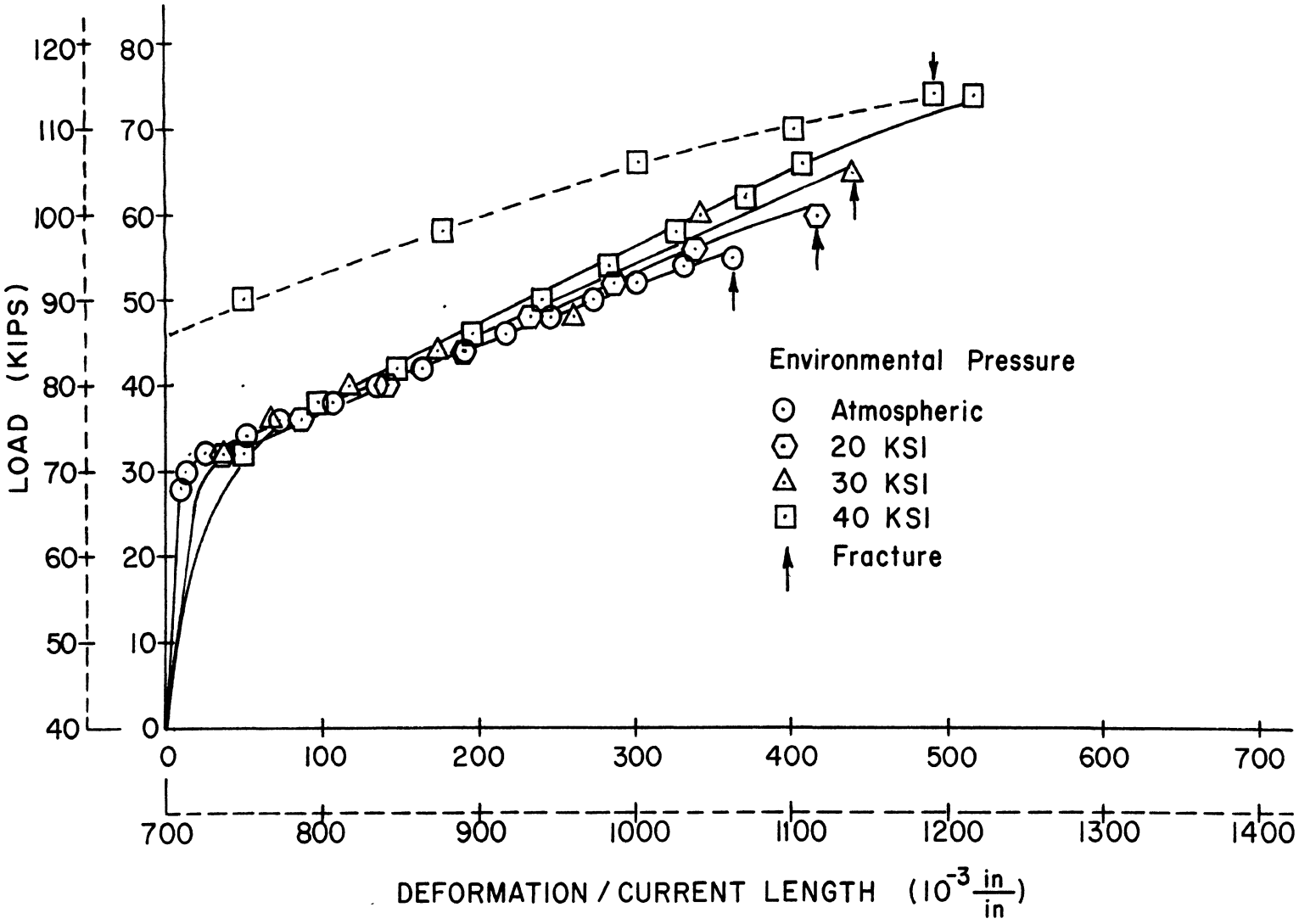

FIG. 8 COMPRESSION TEST (TITANIUM)

they practical when the tests are conducted under a pressurized environment. From the regularity of the curves produced using the parameters of load and deformation per current length it appears that these parameters are useful to use for comparison either between specimens of the same material at different environmental pressures or in comparing specimens of different materials. The similarity between the graph for the compression specimens and the tensile and bending tests is readily apparent. The graphs of the specimens tested in different environmental pressures overlay each other until very large deformations occur. At a load of about 45,000 pounds, the slope of the curves showed a significant increase with increased environmental pressure. This may be material response phenomena but is more likely a combination of geometrical phenomena due to the changing cross-sectional area of the specimen as deformation increases and an increase in load due to an increase in pressure during the test.

The yield stress as determined from the three types of loading fell between 149 ksi and 151 ksi regardless of the environmental pressure at which the test was conducted. There was, therefore, no discernable influence of pressure on the initial yielding of the titanium. Neither did

the environmental pressure significantly alter the material response during inelastic deformation. The only parameters which were obviously affected by the environmental pressure were the fracture stress and the fracture strain. In every type of loading it was found that the stress and strain to fracture was increased by an increase in environmental pressure. The graphs of effective stress versus pressure (Fig. 9) and effective strain versus pressure (Fig. 10) are quite impressive in the clarity with which they show the dependency of fracture on pressure. The relationship for both effective stress and effective strain with pressure is obviously a linear one in the range of pressures at which tests were conducted. The fracture line indicated for titanium in Figure 9 is relatively flat indicating that a change of load paths produced by superimposing an additional load would not gain a designer very much in avoiding fracture. That conclusion, however, is an invalid one and indicates the sort of error which can be encountered by considering effective stress versus pressure without also considering effective strain versus pressure. Figure 10 indicates that a small increase in pressure causes a substantial increase in fracture strain. This additional ductility

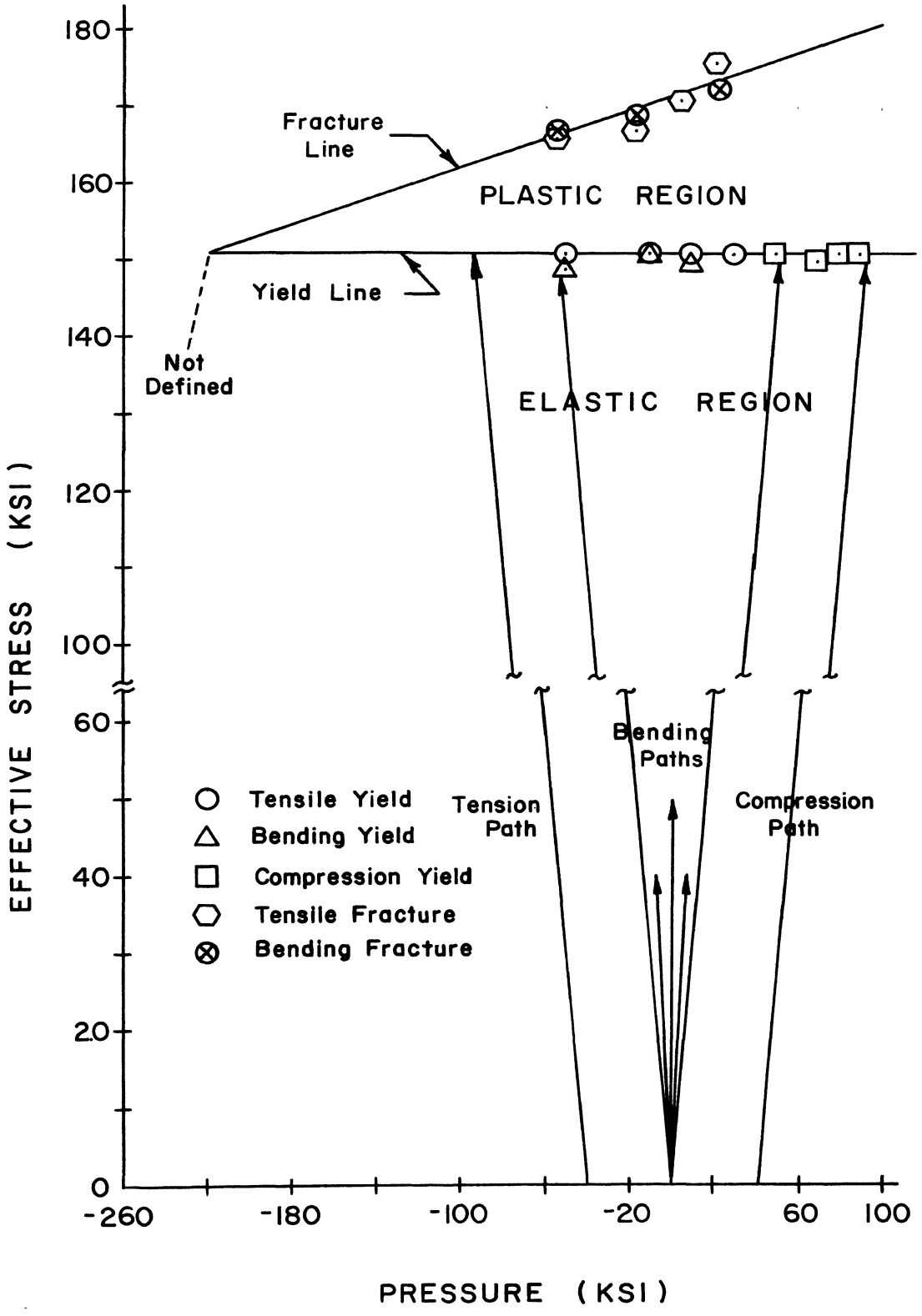

FIG. 9 EFFECTIVE STRESS vs PRESSURE (TITANIUM)

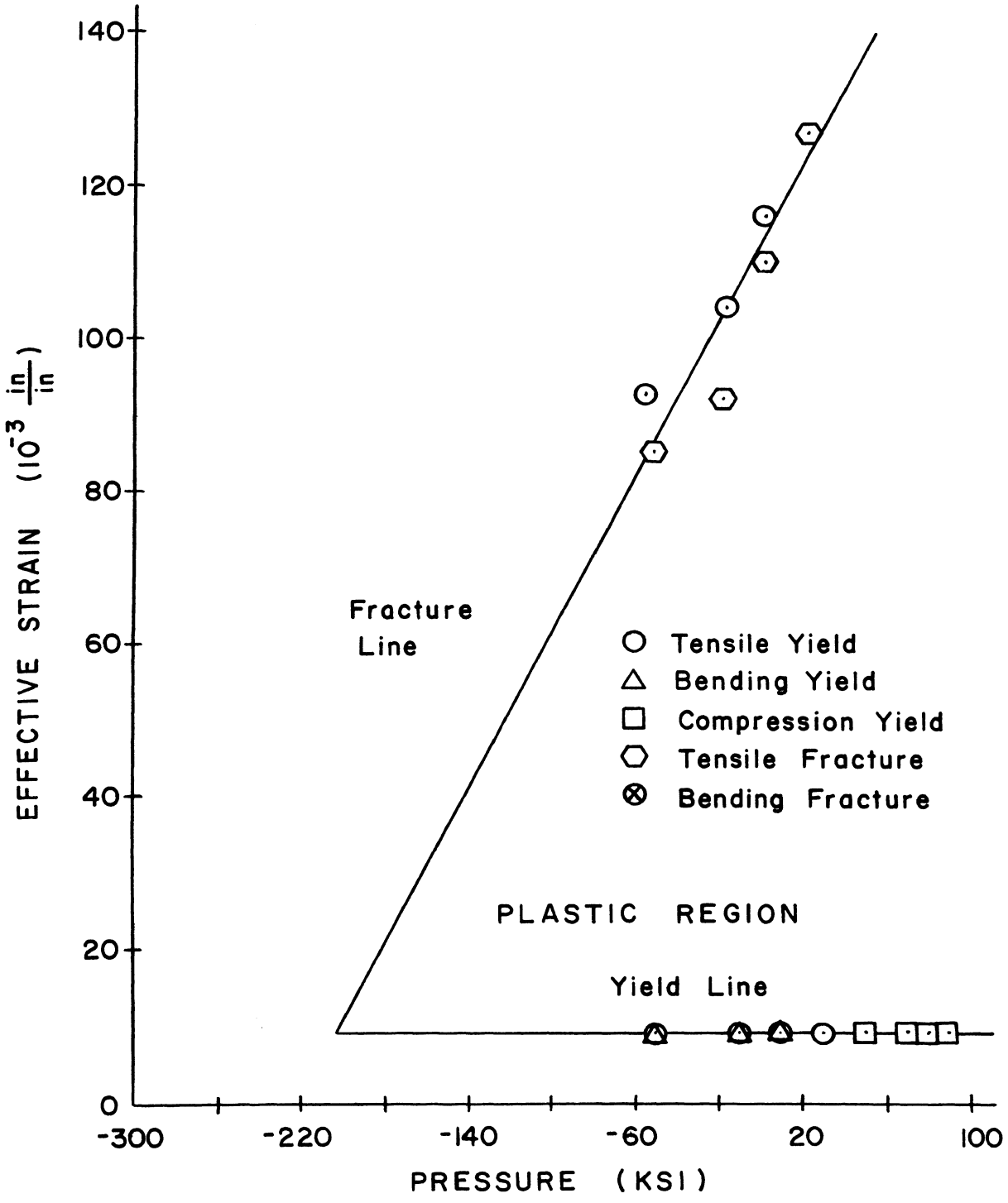

FIG. 10 . EFFECTIVE STRAIN vs. PRESSURE (TITANIUM)

may very well allow the stress in a structure to be redistributed and thereby preventing fracture. This phenomenon provides very useful information for many engineering design procedures concerning large inelastic deformations such as are required in wire drawing, extrusion, or the folding of plates about a small radius die.

The existence of the functional relationship demonstrated in Figure 9 and Figure 10 is of obvious value when the deformation or forming of a machine part is conducted in a hydrostatic environment such as is used in hydrostatic wire drawing or in hydrostatic extrusion with or without back pressure. The value of this relationship is, however, far more general than just the applications to high pressure forming. It can be seen by examining these graphs (Fig. 9 and Fig. 10) that even if the forming is done in an atmospheric environment where the initial environmental pressure is 0 psi that if the load path could be altered in the correct direction a piece could be loaded to a greater effective stress and deformed to a greater effective strain. As a simple example of how this theory could be used let us take a shaft being deformed in pure shear. If the shaft were made of titanium and loaded in an atmospheric environment it would fracture when an

effective stress of 222 ksi is reached, and a corresponding effective strain of .126 in/in. If, however, a load were superimposed on the shear stress so the load path changed from vertical to a slope of plus seven the fracture stress is 229 ksi and the fracture strain is .1486 in/in. This represents a simultaneous increase in strength and ductility of 3.2 and 17.9 per cent respectively. A load path slope of plus seven can be obtained if the following normal stresses are superimposed on the shear stress (Fig. 11)

$$\sigma_x = |\tau_{xy}| \text{ psi T}$$

$$\sigma_y = .75\ |\tau_{xy}| \text{ psi C}$$

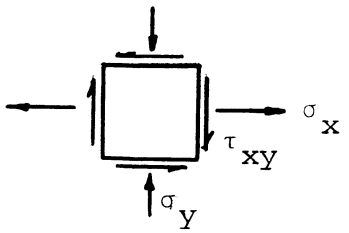

Fig. 11 Superimposed Stresses

B. 7075-T6 Aluminum

(1) Tension - Tension tests were conducted on the aluminum at pressures of 0 ksi, 40 ksi and 70 ksi (Fig. 12). The elastic portion of the stress-strain curves in tension were virtually identical up to the yield point. The modulus of elasticity of the material at all environmental pressures was approximately 9,800 ksi although there was a slight elevation of the yield point as the pressure was increased. In the post-yield portion of the graph there exists a rather interesting

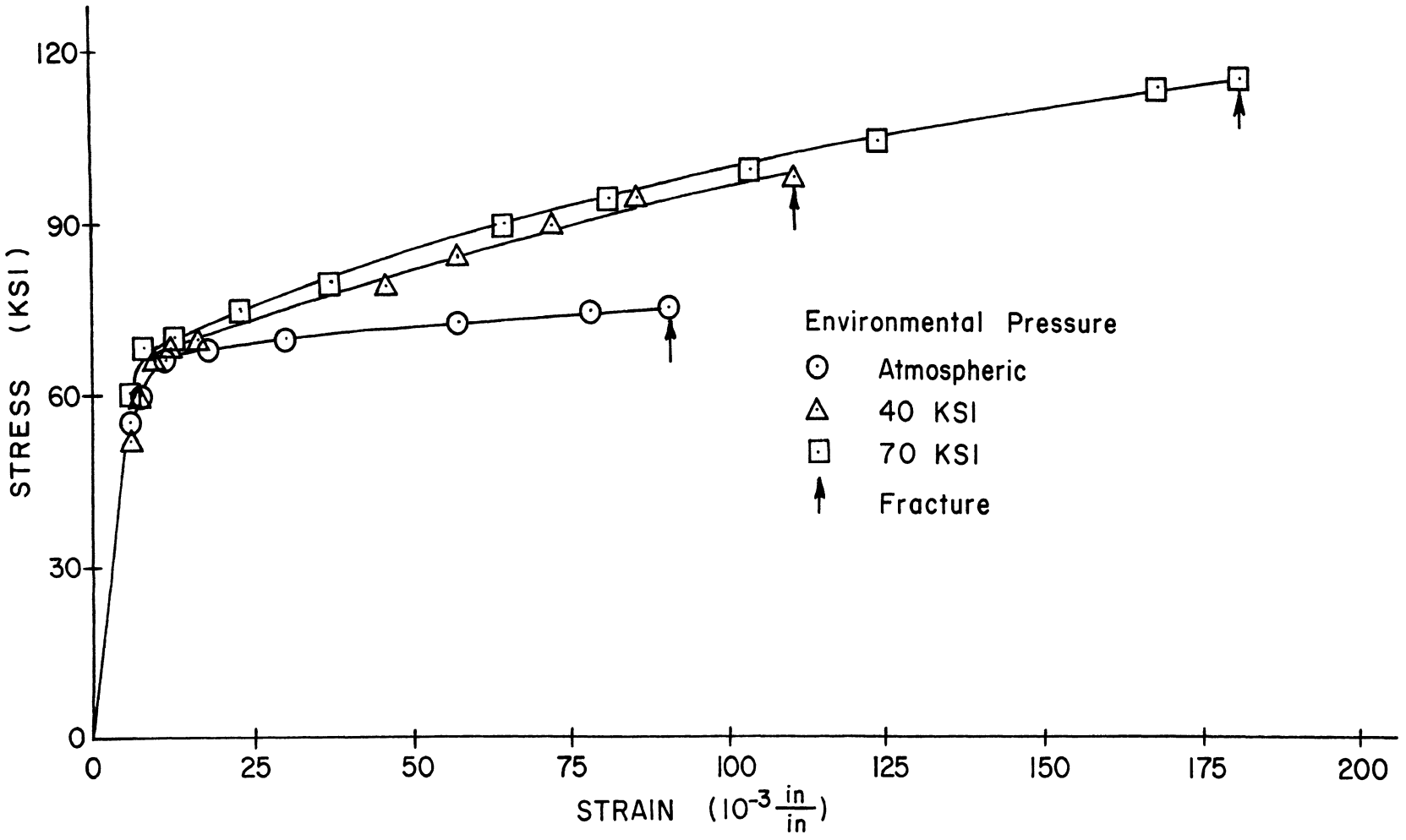

FIG. 12 TENSION TEST (7075-T6 ALUMINUM)

phenomena as we see the slope of the atmospheric test to be markedly flatter than the slope of the tests conducted at elevated pressures. It was suggested to this author by Dr. Bobrowsky that a similar phenomena had been observed in rocks and had been attributed to surface imperfections. For this reason electron microscope photographs were taken at the UMR Materials Research Center (Fig. 13 and Fig. 14). These photographs were taken of the surfaces of both titanium and the aluminum at a magnification of 1,000. Both surfaces were examined so the titanium could act as a control since the titanium did not exhibit this change of slope and was, therefore, assumed to have a significantly different surface finish than the aluminum. The photographs taken using the electron microscope prove to be highly indicative, but inconclusive in proving this theory. From a casual observation of the appearance of the two surfaces it seems obvious that the aluminum is far rougher than the titanium. Surface roughness, however, would probably not be sufficient to cause the phenomena being discussed but a rough surface in conjunction with microscopic surface cracks would. There appear to be several dark areas on the surface of the aluminum indicative of surface cracks. The problem in

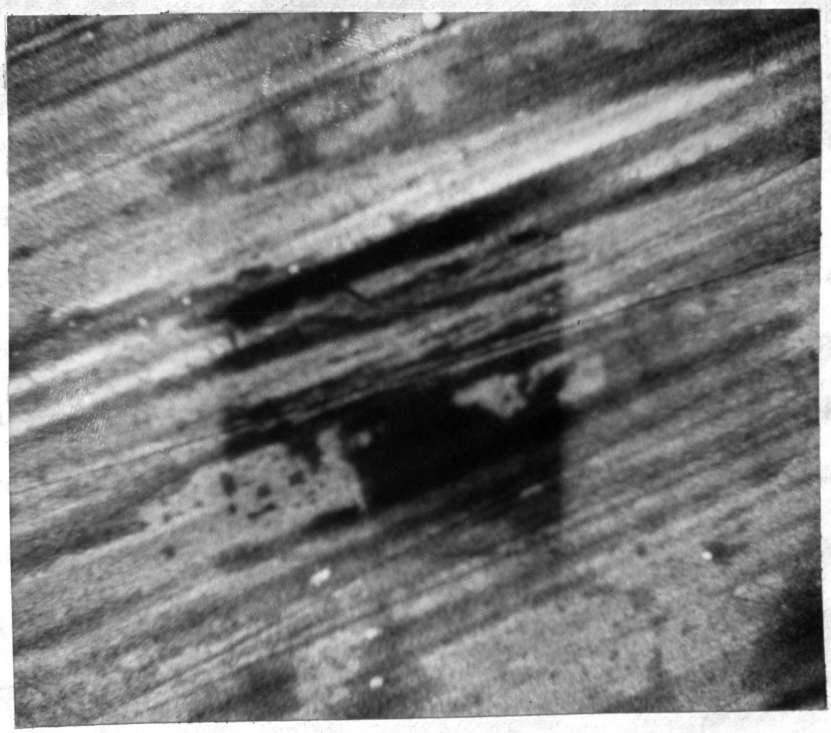

Fig. 13 Electron Micrograph (Titanium)

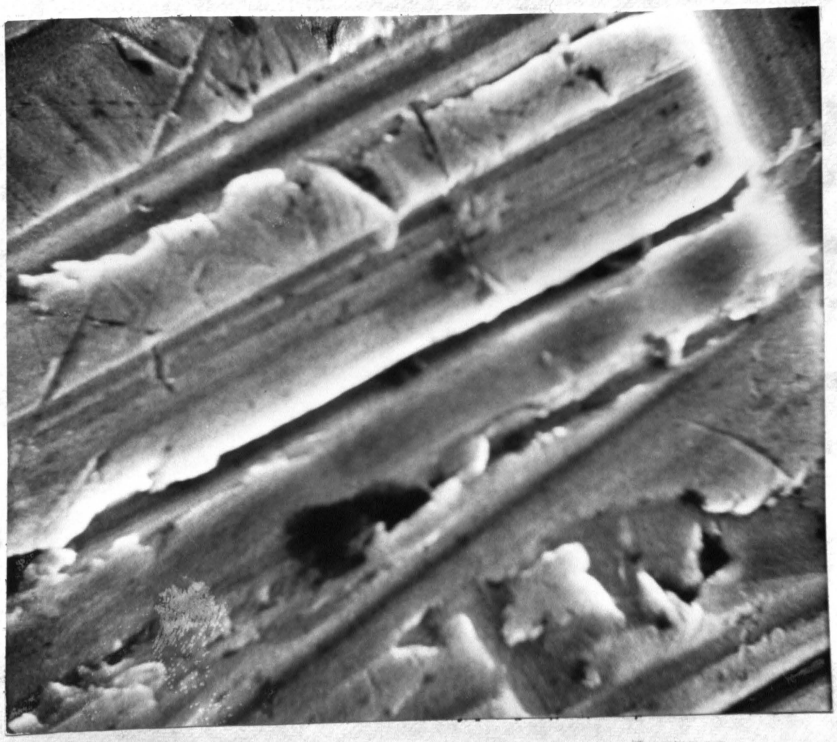

Fig. 14 Electron Micrograph (7075-T6 Aluminum)

interpreting accurately both photographs exists because of the presence of oxides on each material. The oxides of both aluminum and titanium form so rapidly that no photograph was taken of the surfaces without the presence of oxide. It is very common for microscopic quantities of gases to be present during the production of aluminum and thereby produce the sort of microscopic cracks being discussed[18]. The author of this thesis suggests that the flatter slope found when conducting tension tests in atmospheric environments, while not conclusive, is very probably due to microscopic surface cracks. It should be noted that the same phenomena was observed in the bending tests where the strain gage was located on the tension side of the plate indicating that the characteristic is consistently present. The slope of the two tensile specimens tested in elevated pressure environments are virtually parallel. The increased stress required to produce a given amount of strain in the inelastic region for the 40 ksi and 70 ksi environments compared to the atmospheric environment would be due to the tendency of the fluid under pressure to close or "heal" the microscopic cracks. This "healing" of the microscopic cracks would be expected to be far less observable in the compression tests until

barrelling has become sufficiently pronounced for high circumferential deformations to exist in the specimen. This is exactly what was observed (Fig. 15). The existence of a high pressure environment seems to have an affect similar to strain hardening in all three types of loading used.

(2) Bending - Bending tests were conducted at environmental pressures of 0 ksi, 20 ksi, and 40 ksi (Fig. 16). For the same reason as was given in the discussion of titanium bending tests the parameter of load was used in making the graph rather than stress. The major characteristics of the family of curves produced by the bending tests are the same as those produced by the tension tests. The elastic region was essentially unaffected by the environmental pressure at which the test was conducted. The yield stress was increased with an increase of environmental pressure similar to that shown in the tension test in Figure 12. The yield stresses indicated by the bending tests at elevated pressures were slightly higher than those given by the tension and compression tests even after accounting for the difference in load path. The effective strain at yield, however, was very consistent in bending with the tension and compression test

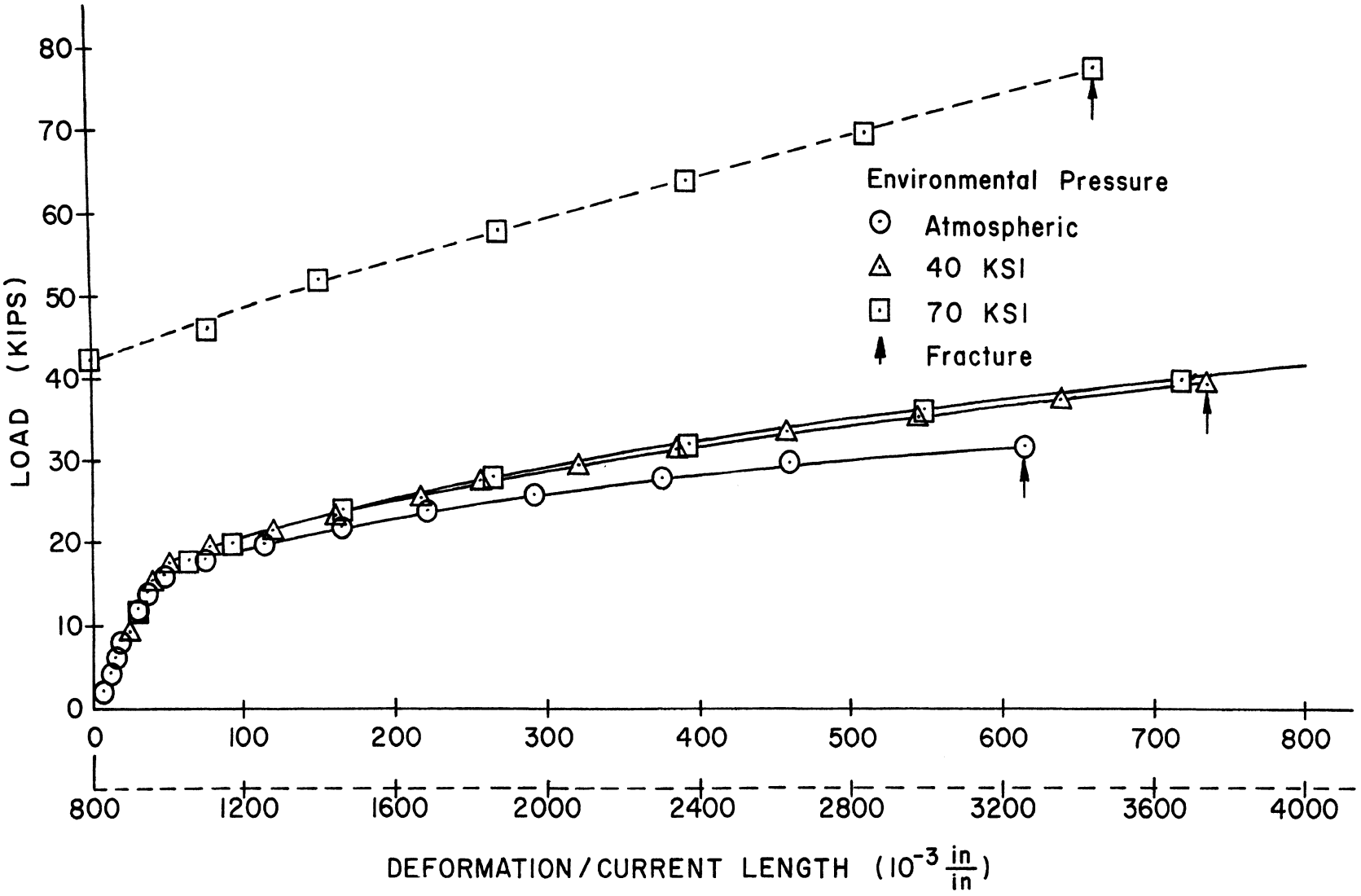

FIG. 15 COMPRESSION TEST (7075-T6 ALUMINUM)

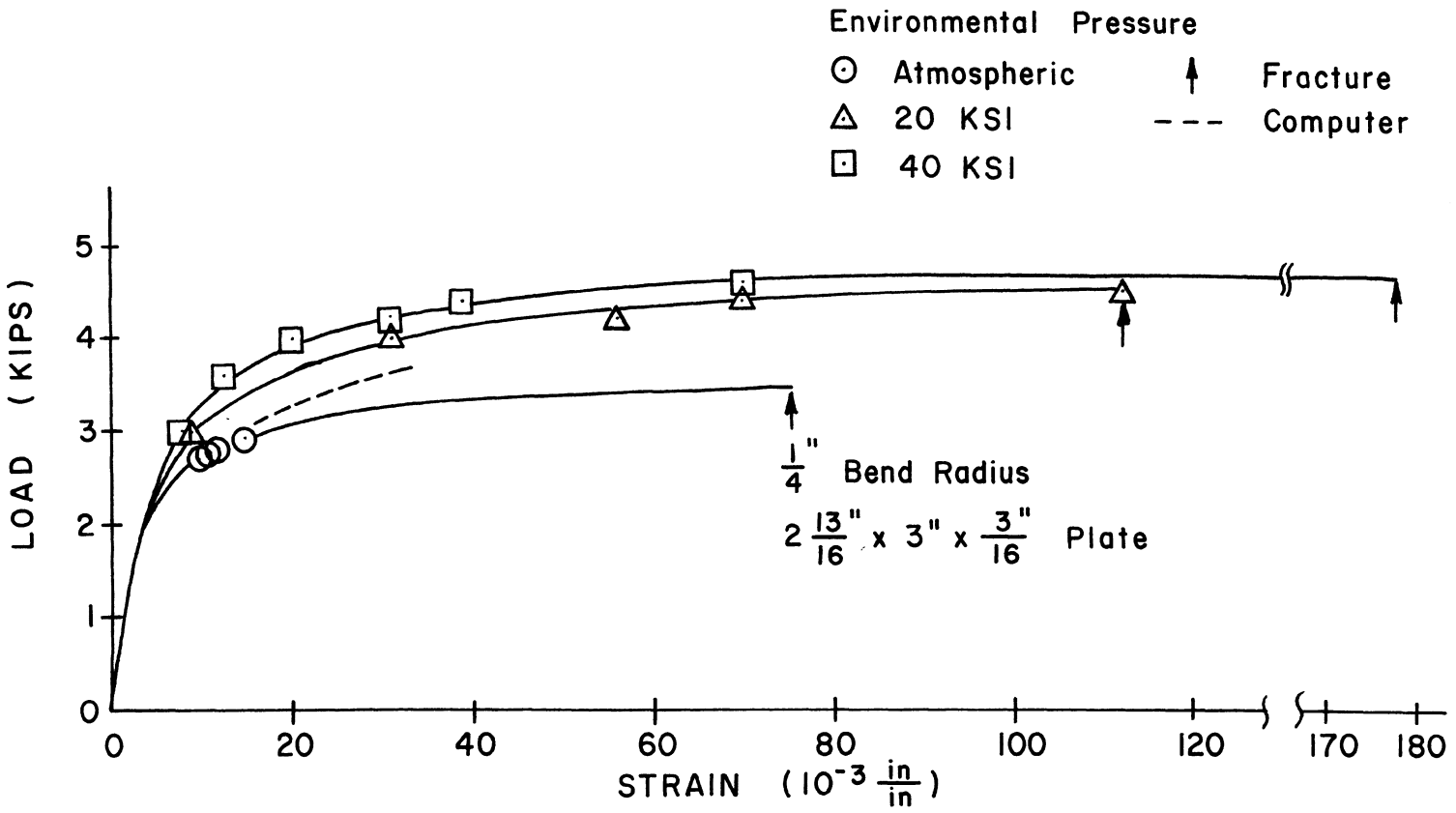

FIG. 16 BENDING TEST (7075-T6 ALUMINUM)

results. The reason for the difference in yield stress in bending is not known and the deviation is not so large as to be disturbing. In all probability the discrepancy is due to an inexact knowledge of the moment arm which should be used in converting the load to stress. This calculation was done using simple beam theory and the error in moment arm would be linearly related to the error in stress. Tension data was used for input into a computer program. The computer program was used to predict the behavior of the folded plate for both materials. The results obtained from the computer analysis were very useful but not nearly as satisfying as the ones from the titanium which virtually duplicated the experimental data. The reason for the slightly less accurate results for the aluminum is attributed to the more complicated tensile stress-strain curve which was used as input to describe the inelastic response of the material. The aluminum tension stress-strain curve had a typical yield region where the curve was much more rounded while with the titanium the transition from elastic to inelastic was very sharp.

(3) Compression - Compression tests were conducted in environmental pressures of 0 ksi, 40 ksi, and 70 ksi (Fig. 15). The modulus of elasticity in

compression was the same as in tension within experimental accuracy. The modulus of elasticity was independent of the environmental pressure at which the test was conducted. The graph was plotted using load versus deformation per current length as parameters for the same reason as the titanium compression specimens. The similarity of the compression tests to the tension and bending tests in the inelastic portion of the curves are very pleasing in that they indicate that the information which can be obtained from these graphs are in fact true material responses and not some unknown factor inadvertently introduced.

C. General Discussion of Experimental Results

The effective stress, effective strain, and pressure was calculated for each of the tests conducted and plotted on the graphs of effective stress versus pressure (Fig. 17) and effective strain versus pressure (Fig. 18). The slope of the load path for a tensile test is easily calculated to be minus three and that for a compression test plus three. Using this information and assuming that the plate being folded in the bending test was in uniaxial tension on the tension side of the plate all of the way to fracture, these graphs are easily plotted. The state of stress and strain in a compression specimen after large deformation and barrelling have taken place are unknown and could not be included on the graphs. The yield stress and the yield

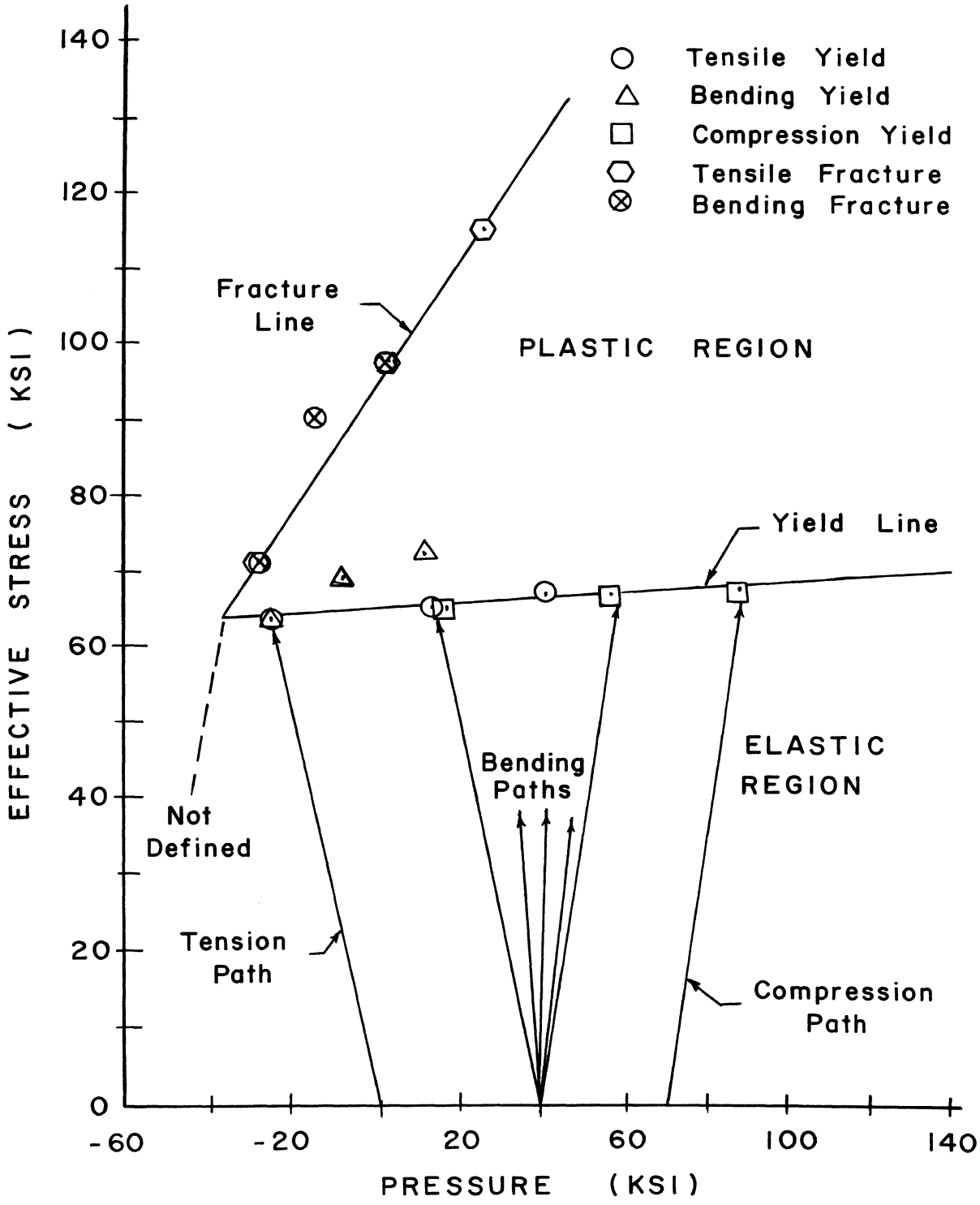

FIG. 17 EFFECTIVE STRESS vs. PRESSURE (7075-T6 ALUMINUM)

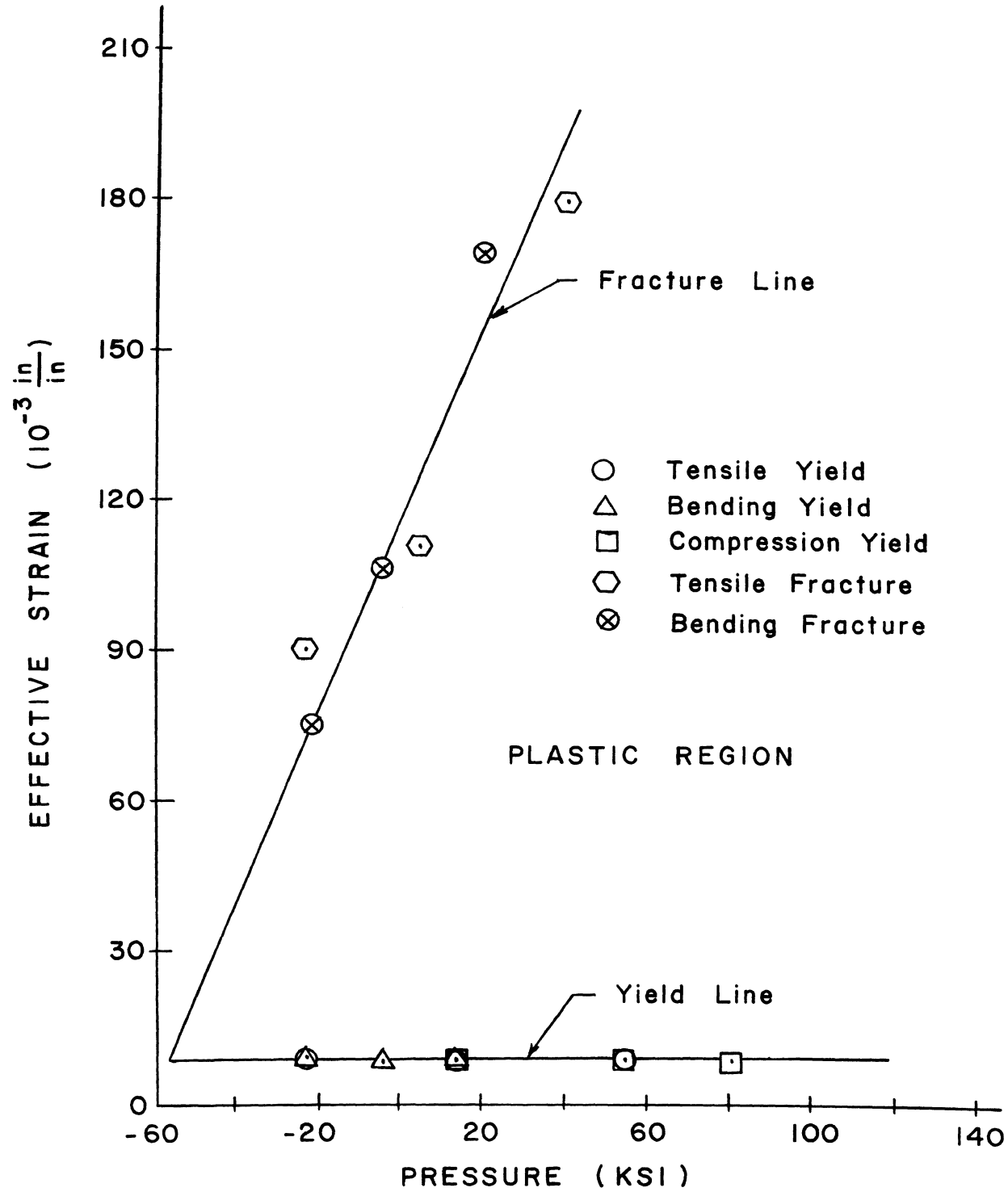

FIG. 18 EFFECTIVE STRAIN vs. PRESSURE (7075-T6 ALUMINUM)

strain could, of course, be calculated for each of the three loading conditions and were included on the graphs of Figures 17 and 18. The general appearance of the effective stress versus pressure and effective strain versus pressure for the 7075-T6 aluminum is very similar to that for the titanium. It is apparent that the environmental pressure does affect yielding of the aluminum and the influence is quite linear within the range of pressures investigated. There is a projected intersection of the yield and fracture line at which yield and fracture would be expected to occur at the same stress. To experimentally confirm this using simple stress states in which we have a great deal of confidence would require superimposing a hydrostatic tensile pressure to the uniaxial tension specimen. Neither the author of this thesis nor anyone in the literature has devised a satisfactory method to accomplish this so a confirmation of this prediction was not achieved. The fracture stress and the fracture strain also apparently varies linearly with the environmental pressure and with a far steeper slope than was indicated on the titanium. This of course means that any forming operation on the aluminum carried out in a high pressure environment could be designed to produce substantially greater stresses and strains without fracturing than the same operation performed in an atmospheric environment. The steeper slope of the fracture line further indicates that the load path used to produce a desired deformation would be very significant in reducing the probability of fracture.

Using the same example that was used for titanium in illustrating the advantages inherent in the effective stress versus pressure graph and the effective strain versus pressure graph we can readily observe the significance of the slope of the stress fracture line and the strain fracture line. The example used was a comparison between a shaft being loaded in pure shear, which would produce a vertical load path on the effective stress versus pressure graph, and a shaft loaded in shear with normal stresses superimposed which produce a slope of plus seven for the load path (Fig. 11). The specimen with a vertical load path would fracture with an effective stress of 146 ksi and with an effective strain of 0.161 in/in. If the slope of the load path on the effective stress versus pressure curve is plus seven the effective stress at fracture is 181 ksi and the effective strain at fracture is 0.218 in/in. The pressure that would exist at fracture would be 25 ksi. This change in load path, therefore, produces an increase in fracture strength of 24 per cent and an increase in fracture strain of 35.4 per cent. These results are tabulated in Table I.

There are some aspects of the graphs (Figs. 17 and 18) which remain unknown until further experiments are conducted. It is probable that the fracture line does not remain linear but changes slope at a sufficiently high pressure or for a sufficiently positive load path. This is surmised because of work done by Bridgman[1] and Davis[2].

TABLE I

	VERTICAL LOAD PATH		LOAD PATH SLOPE OF 7		PER CENT INCREASE	
	σ_e(ksi)	ε_e(in/in)	σ_e(ksi)	ε_e(in/in)	σ_e	ε_e
Aluminum	146	.161	181	.218	24.0	35.4
Titanium	222	.126	229	.1486	3.2	17.9

TABLE I. Influence of Load Path on Fracture

The data for all of the tests reported on in this thesis are tabulated in Table II. For a uniaxial load the effective stress and the uniaxial stress are identical and the pressure is one-third of the uniaxial stress so the slope of the curve is ± three depending on whether the uniaxial stress is tensile or compressive. Since pressure is defined as minus J_1 a compressive stress gives a positive slope. It was assumed that all of the stresses were uniaxial up to the fracture load. From the definition of effective strain we find that the effective strain is identical in magnitude to the axial strain. From a tabulation such as Table II it is relatively simple to compose a tertiary plot of effective stress versus effective strain versus pressure which incorporates the three invariant parameters assumed to describe the material response. Such graphs are shown in Figures 19 and 20. The general shape of these two graphs are such as to indicate that fracture is unquestionably a function of the first invariant, or pressure, and that relationship is a very simple linear one for these materials within the range of pressures investigated. The nature of the graph of both aluminum and titanium is similar to that indicated by Davis[2] for Nittany No. 2 brass. The author of this thesis believes that these results are highly indicative that a graph of similar nature exists for many or possibly all common structural metals. It is believed that the graphs will prove linear for body centered cubic and face centered cubic materials although the relationship will probably be

TABLE II

Type of Load	Environmental Pressure (ksi)	Yield σ_e (ksi)	Yield Pressure (ksi)	Yield ε_e (in/in)	Fracture σ_e (ksi)	Fracture Pressure (ksi)	Fracture ε_e (in/in)
			TITANIUM				
Tension	0	151	-50.3	0.0089	166	-55.3	.085
Tension	40	151	-10.3	0.0089	167	-17.7	.092
Tension	60	151	+ 9.7	0.0089	171	+ 3.0	.110
Tension	80	151	+29.7	0.0089	176	+21.5	.127
Bending	0	149	-49.7	0.0088	167	-55.7	.0916
Bending	40	151	-10.3	0.0089	169	-16.3	.104
Bending	60	150	+ 9.6	0.0088	173	+ 3.5	.116
Compression	0	151	+50.3	0.0089			
Compression	20	150	+70.0	0.0088			
Compression	30	151	+80.3	0.0089			
Compression	40	151	+90.3	0.0089			
			ALUMINUM				
Tension	0	64	-25.0	.0080	71	-28.0	.090
Tension	40	65	+14.0	.0080	98	+ 3.0	.110
Tension	70	67	+42.0	.0080	116	+27.0	.180
Bending	0	64	-25.5	.0080	71	-28.0	.075
Bending	20	69	- 8.0	.0080	91	-14.0	.105
Bending	40	72	+12.0	.0080	98	+ 3.0	.170
Compression	0	65	+18.0	.0080			
Compression	40	67	+58.0	.0080			
Compression	70	68	+90.0	.0080			

TABLE II. Tabulation of Yield and Fracture Data

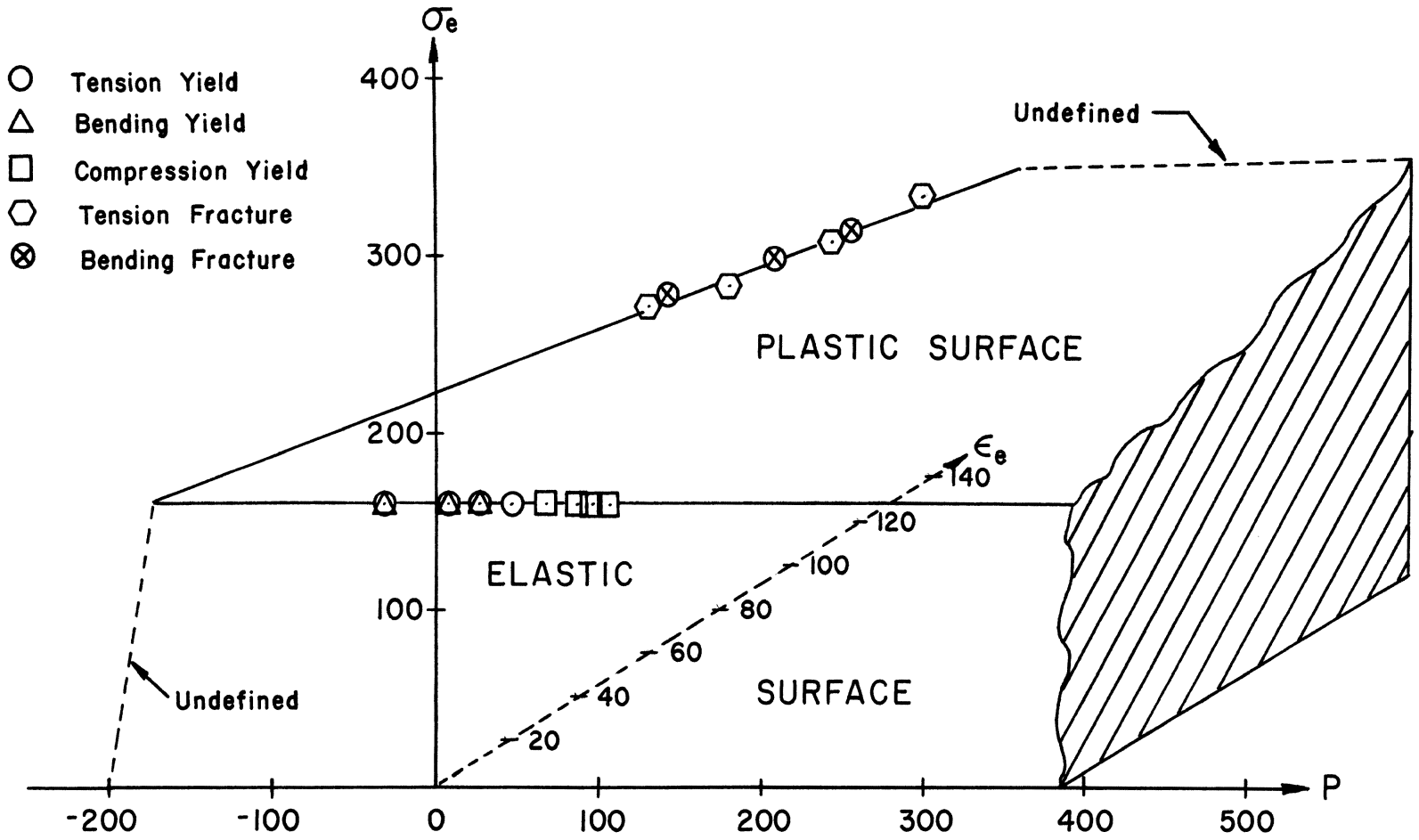

FIG. 19 YIELD AND FRACTURE MODEL FOR TITANIUM

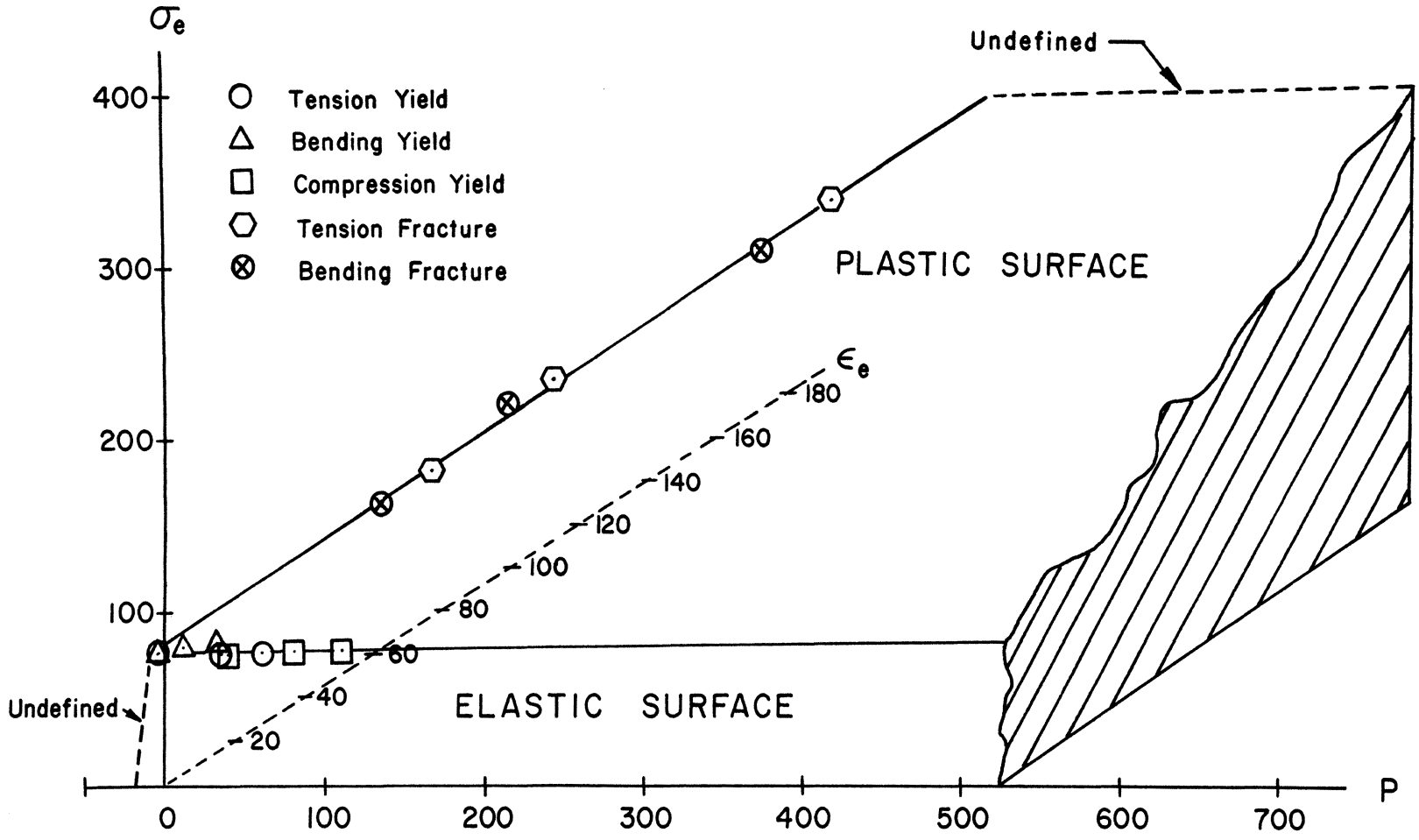

FIG. 20 YIELD AND FRACTURE MODEL FOR 7075-T6 ALUMINUM

nonlinear for some face centered cubic materials and most hexagonal close packed materials. The justification of the preceeding statement is based partly on evidence and partly on a very loosely formed concept held by this author. Dr. Bobrowsky[7] has shown that the relationship for beryllium, which is a HCP material, is nonlinear. With this in mind it seems logical that the smaller number of slip planes that exist in a material the less random will be the macroscopic effect of the parameters which induce inelastic deformation and ultimately fracture. It has been rather conclusively shown that effective stress, effective strain, and pressure are related parameters which can be used to describe yielding and fracture.

An interesting relationship was discovered while examining the thin plates. The strain in the titanium plates was measured almost to fracture and the uncertainty in the strain at fracture was small. This was not true for the aluminum plates, however, and it was necessary to extrapolate the bending curves and estimate the fracture strain. It seemed desirable to find an alternate and independent method of calculating the strain at fracture if possible. It is well known from fundamental beam theory that the strain is directly proportional to the distance from the neutral axis and inversely proportional to the radius of curvature. This relationship is dependent on plane cross sections remaining plane which in turn primarily depends on shear distortion being negligible. It was decided to calculate the

radius of curvature of the plate in the vicinity of the fracture and from this to calculate the fracture strain. The results obtained agreed with the data extremely well. It should be pointed out that this should not be expected to be a generally reliable relationship but is apparently valid for the type of loading which was imposed on these plates. A comparison of the values of the fracture strain as obtained from data and as calculated is given in Table III. The data graphed and tabulated in Table II was obtained from single tests. Several duplicate tests were conducted to ascertain the reproducibility of the tests. In each case the reproducibility was very good.

TABLE III

Material	Pressure ksi	Fracture Strain From Data in/in	Fracture Strain From Calculation in/in	Per Cent Difference
Aluminum	0 ksi	.075	.075	0.0
	20 ksi	.112	.1275	12.1
	40 ksi	.170	.182	7.1
Titanium	0 ksi	.0916	.0965	5.3
	40 ksi	.104	.106	1.9
	60 ksi	.116	.120	3.4

TABLE III. Comparison of Fracture Strain from Data and Simple Beam Theory

VII. CONCLUSIONS AND RECOMMENDATIONS FOR FURTHER RESEARCH

The need for the inclusion of the parameter defined as pressure in describing material response during inelastic deformation for the metals reported in this thesis is clearly shown. Since this influence has been shown for a number of materials by various investigators it is felt that pressure should be at least considered for all designs involving inelastic deformations. It is further proposed that the parameters of effective stress, effective strain, and pressure as defined in this thesis are the proper parameters to use in describing this influence. It is believed that the types of tertiary graphs developed and shown in Figures 19 and 20 are sufficiently simple to use, after they have been constructed by researchers, that they could be of great value to any designer, not just high pressure designers. It is further proposed that a few tensile tests conducted at varying environmental pressures are sufficient to construct the graph. The range of pressures desired depends on the range of the graph desired and whether the relationship between the parameters prove linear or nonlinear. If the material has a linear response four tensile tests should prove quite sufficient to construct the graph.

There are two regions of the tertiary graph which were not determined and on which further research could be focused. One of these regions is the nature of the material response in the vicinity of the intersection of the yield

line and the fracture line. It is possible that this region can be explored using finite element programs to determine some loading which produces a large tensile pressure as a part of the stress state. An investigation of various types of notches may prove useful. The other region which was not investigated because of the limitation on maximum permissible pressure on the equipment is the nature of the fracture line at high pressures. It is very likely that the slope of the fracture line does not remain constant but changes abruptly to another, much flatter, slope at some point. This has been indicated by Davis[2] using data from Bridgman[14]. It is now possible to conduct tests at pressures up to 450 ksi on this campus using the Beta Press installed in January, 1972.

A further area of research which could prove very informative would be a schedule of tests conducted at atmospheric pressures using effective stress, effective strain, and pressure as parameters. This schedule of tests would include tension, torsion, plate bending, compression, and combinations of these to determine if the tertiary models of Figures 19 and 20 describe those responses and if those tests might be used to construct the graphs so that expensive pressure apparatus might not be required.

BIBLIOGRAPHY

1. P. W. Bridgman, "Breaking Tests Under Hydrostatic Pressure and Conditions of Rupture", Phil. Mag. 24, pp. 63-80.

2. R. L. Davis, "A Macroscopic Model of Material Behavior Under Variable Pressures", Int. Coll. on the Physics of Solids Under Pressure, Grenoble, France, 1969.

3. L. W. Hu, "Plastic Stress-Strain Relations", ASTIA-AD 266887, 1961.

4. R. Hill, "Plasticity", Oxford University Press, 1950.

5. Hu, Markowitz, and Bartush, "A Triaxial Experiment on Yield Condition in Plasticity", AFOSR Scientific Report No. 65-0313.

6. A. Bobrowsky, "Map-Penntap", Short Course, 1969.

7. A. Bobrowsky, "Pressure Research Notes".

8. H. Ll. D. Pugh, "Hydrostatic Extrusion", Ninth Commonwealth Mining and Metallurgical Congress, 1969.

9. B. Avitzur, "Metal Forming: Processes and Analysis", McGraw-Hill, 1968.

10. J. G. Hoeg and R. L. Davis, "Effects of Cold Working Under Pressure on Subsequent Yield", ASME Paper No. 71-WA/PT-6.

11. W. Prager, "Models of Plastic Behavior", Proceedings of the Fifth U. S. Congress on Applied Mechanics, ASME, 1966, pp. 435-450.

12. R. Hill, "Plasticity", Oxford University Press, p. 34, 1950.

13. Thomsen, Cornet, Lotz, and Dorn, "Investigation of the Validity of an Ideal Theory of Elastic-Plasticity for Wrought Aluminum Alloys", NACA TN 1552, 1948.

14. P. W. Bridgman, "Studies in Large Plastic Flow and Fracture", McGraw-Hill, 1952.

15. Hu and Pae, "The Inclusion of Hydrostatic Stress Component in Yield Condition and Applications", ASTIA-AD 266887, 1961.

16. T. C. Hsu, "Materials Research and Standards", MTRSA, Vol. 9, No. 12, p. 20.

17. C. V. Girijavallabhan and K. C. Mehta, "Stress-Strain Relationship from Compression Tests on Nonlinear Materials", 3-Dimensional Finite Element Symposium, Vanderbilt University, Fall, 1969.

18. A. S. Tetelman and A. J. McEvily, Jr., "Fracture of Structural Materials", pp. 421-424, John Wiley and Sons, Inc., 1967.

19. A. Mendelson, "Plasticity: Theory and Application", MacMillan Company, 1968.

VITA

Richard L. Pendleton, the son of Mr. and Mrs. Clarence Pendleton was born September 5, 1935, in Jefferson City, Missouri.

He received his primary and high school education in Owensville, Missouri. After attending Southwest Baptist College in Bolivar, Missouri his freshman year he transferred to Missouri School of Mines and Metallurgy and completed requirements for a Bachelor of Science Degree in Mechanical Engineering in May, 1957.

Mr. Pendleton was employed as a Natural Gas Engineer by Socony Mobil Oil Company until August, 1962, at which time he accepted an instructorship in the Engineering Mechanics Department at the University of Missouri - Rolla. He enrolled in the Graduate School at the University of Missouri - Rolla in September, 1962, and completed requirements for a Master of Science Degree in Mechanical Engineering in May, 1965.

He was married to Miss Lavon Byrd on February 15, 1958, and has four children, Richard Brian, Linda Kay, Rebecca Lavon, and David Randall.

APPENDIX A.

SOLUTION OF A SIMPLY SUPPORTED BEAM USING LARGE DISPLACEMENT THEORY

The finite element computer program used for analyzing the folded beam was one written as a Masters Thesis by Vernon Allen, UMR, 1971. The title of the thesis was "Development of an Elastic-Plastic Finite Element Program with the Initial Strain Approach". In this program the method of successive elastic solutions[19] was employed and the problem of nonconvergence for perfectly plastic problems was eliminated by expressing the Prandtl-Ruess equations entirely in terms of strain. The stress-strain curve used with this program was bilinear for titanium and had four sectionally continuous linear regions for aluminum. The formulation of this program did not include rotations due to shear for large deformations and, therefore, became invalid when the plate was folded through large rotations.

It is suggested by the following theoretical development that it is possible to combine simple beam theory with large displacement theory from continuum mechanics and arrive at a solution which will describe the response of a beam when large inelastic deformations are present. The beam is assumed to be of length 2L, height h, and unit width. The beam is simply supported at each end and has a point load applied at the center (Fig. A1). The uniaxial stress-strain diagram for the material is shown in Figure A2.

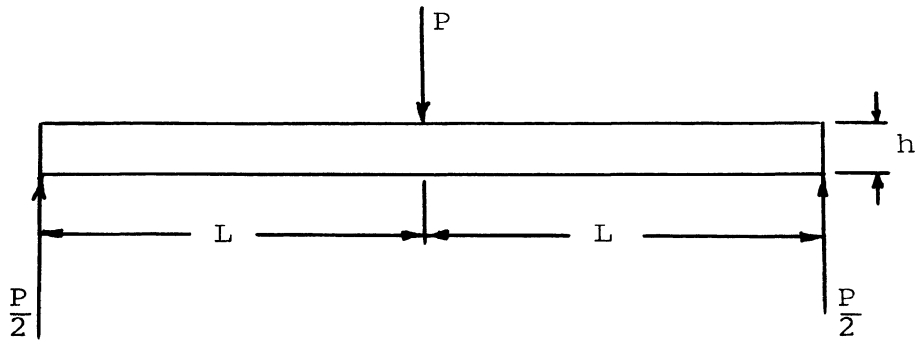

Fig. A1 Beam Load Diagram

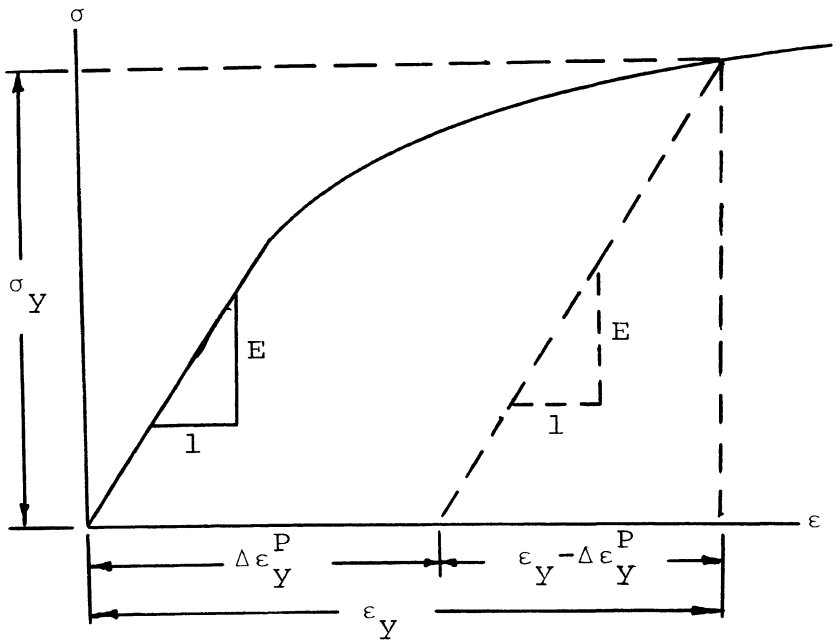

Fig. A2 Uniaxial Stress-Strain Diagram

where:

σ_y = Normal stress in the y direction.

ε_y = Total normal strain in the y direction.

$\Delta\varepsilon_y^P$ = Total plastic normal strain in the y direction.

The origin of a conventional cartesian coordinate system is placed at the geometric center of the beam and a free body diagram is taken of the right end as shown in Fig. A3.

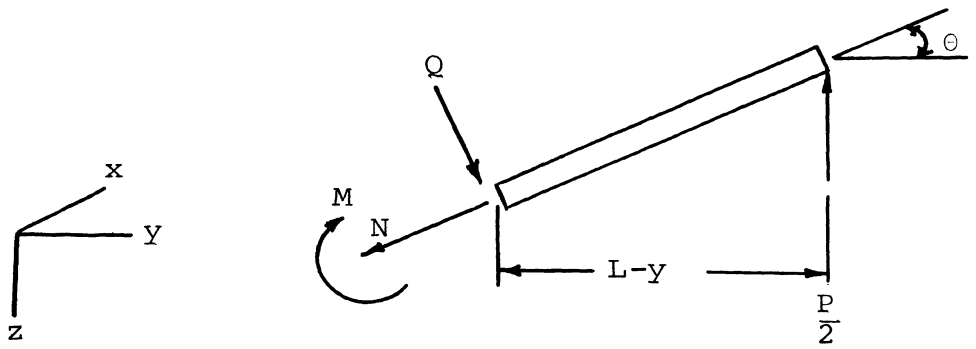

Fig. A3 Free Body Diagram

The internal reactions at an arbitrary position y are:

N = Force per unit width normal to the cross section.

Q = Force per unit width parallel to the cross section.

M = Internal moment per unit width about the z axis.

From equilibrium conditions it can be shown that

Eq. 1A $N = \frac{P}{2} \text{Sin } \theta$

Eq. 2A $Q = \frac{P}{2} \text{Cos } \theta$

Eq. 3A $M = \frac{P}{2} (L - y)$

The internal force N can be related to the stress distribution in the following conventional manner:

$$\text{Eq. 4A} \qquad N = \int_{-\frac{h}{2}}^{\frac{h}{2}} \sigma_y dz = \int_{-\frac{h}{2}}^{\frac{h}{2}} E(\varepsilon_y - \Delta\varepsilon_y^P) dz$$

Let us define

$$\text{Eq. 5A} \qquad \int_{-\frac{h}{2}}^{\frac{h}{2}} E\Delta\varepsilon_y^P dz = E\Theta_o$$

and Eq. 4A becomes

$$\text{Eq. 6A} \qquad N = \int_{-\frac{h}{2}}^{\frac{h}{2}} E\varepsilon_y dz - E\Theta_o$$

In a similar manner the internal moment can be expressed as

$$\text{Eq. 7A} \qquad M = \int_{-\frac{h}{2}}^{\frac{h}{2}} \sigma_y z dz = \int_{-\frac{h}{2}}^{\frac{h}{2}} E(z\varepsilon_y - z\Delta\varepsilon_y^P) dz$$

Let us define

$$\text{Eq. 8A} \qquad \int_{-\frac{h}{2}}^{\frac{h}{2}} Ez\Delta\varepsilon_y^P dz = E\Theta_1$$

and Eq. 7A becomes

$$\text{Eq. 9A} \quad M = \int_{-\frac{h}{2}}^{\frac{h}{2}} Ez\varepsilon_y dz - E\Theta_1$$

From continuum mechanics it can be shown that

$$\text{Eq. 10A} \quad \varepsilon_y = V_y + \frac{1}{2}(V_y^2 + w_y^2) \simeq V_y + \frac{1}{2} w_y^2$$

where

V = Displacement in the y direction

w = Displacement in the z direction

and the subscript y refers to a derivative with respect to y. The $\frac{1}{2} V_y^2$ term in this problem is assumed to be negligible compared to the other terms. It can further be shown that

$$\text{Eq. 11A} \quad V = \bar{V} - zw_y$$

where $\bar{V}$ is the y displacement of the neutral axis. Combining Eqs. 10A and 11A to obtain

$$\text{Eq. 12A} \quad \varepsilon_y = \bar{V}_y - zw_{yy} + \frac{1}{2} w_y^2$$

Substituting Eq. 12A into Eqs. 6A and 9A we obtain

$$\text{Eq. 13A} \quad N = E\bar{V}_y h + \frac{E}{2} w_y{}^2 h - E\Theta_o$$

and

$$\text{Eq. 14A} \quad M = -\frac{Eh^3}{12} w_{yy} - E\Theta_1$$

Equate Eq. 14A and Eq. 3A to obtain

$$\text{Eq. 15A} \quad w_{yy} = -\{\frac{P}{2}(L - y) + E\Theta_1\} \frac{12}{Eh^3}$$

Integrate Eq. 15A twice to obtain

$$\text{Eq. 16A} \quad w_y = -\{\frac{P}{2}(Ly - \frac{y^2}{2}) + E\Theta_1 y\} \frac{12}{Eh^3} + C_1$$

$$\text{Eq. 17A} \quad w = -\{\frac{P}{2}(\frac{Ly^2}{2} - \frac{y^3}{6}) + \frac{E\Theta_1 y^2}{2}\} \frac{12}{Eh^3} + C_1 y + C_2$$

There are two boundary conditions which may be used to evaluate the constants of integration. They are:

No. 1 $\quad w_y = 0 \quad$ at $\quad y = 0$

No. 2 $\quad w = 0 \quad$ at $\quad y = L$

From boundary condition No. 1

$$\text{Eq. 18A} \quad C_1 = 0$$

From boundary condition No. 2

$$\text{Eq. 19A} \quad C_2 = \frac{2L^2}{Eh^3} (PL + 3E\Theta_1)$$

Equate Eqs. 1A and 13A and solve for $\bar{V}_y$ to obtain

$$\text{Eq. 20A} \quad \bar{V}_y = \frac{1}{Eh} \{\frac{P}{2} \text{Sin } \theta - \frac{1}{2} w_y{}^2 h + E\Theta_o\}$$

Computing Procedure:

(1) Set load increment P.

(2) Set initial values of Θ_o and Θ_1 at zero.

(3) Calculate ε_y.

  (a) Calculate w with Eq. 17A

  (b) Calculate w_y with Eq. 16A

  (c) Calculate w_{yy} with Eq. 15A

  (d) Calculate $\bar{V}_y$ with Eq. 20A

  (e) Calculate ε_y with Eq. 12A

(4) Check for yielding and calculate $\Delta\varepsilon_y^P$ by Mendelson's[19] method.

(5) Calculate Θ_o and Θ_1 using Eqs. 5A and 8A.

(6) Iterate steps 3 through 5 until ε_y converges.

(7) Increment load and repeat steps 2 through 6.

The load could be incremented until the load which would be expected to initiate fracture is reached. A computer subroutine could be included which would calculate the stress, strain, displacement, effective stress, effective strain, and pressure for any point in the beam at any desired applied load.